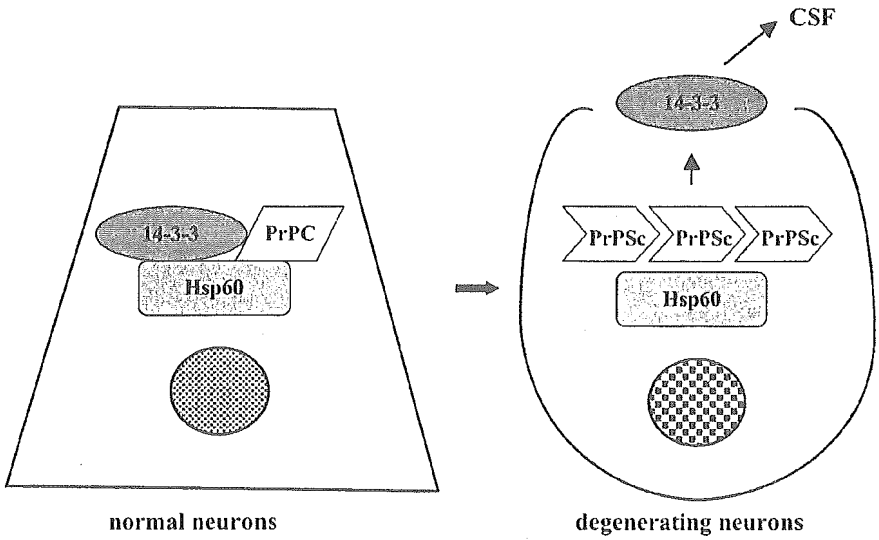

FIGURE 9. A possible mechanism for elevation of 14-3-3 protein in the cerebrospinal fluid of prion diseases. When affected with the pathogenetic prion, the molecular complex composed of 14-3-3, Hsp60, and PrPC becomes disintegrated during the conversion of PrPC into PrPSc aggregates, which displace the 14-3-3 protein from the complex, resulting in the release of 14-3-3 from degenerating neurons into the cerebrospinal fluid.

protein overlay analysis. These observations indicate that the 14-3-3 protein forms a molecular complex with Hsp60 and PrPC in the human CNS.

PrPC is a glycosylphosphatidylinositol (GPI) anchored cell-surface protein, expressed at highest levels in neurons and at substantial levels in astrocytes in the CNS (28, 29). Although a low level of extramitochondrial coexpression could not be excluded, the present study showed the substantial colocalization of 14-3-3, Hsp60, and PrPC in the mitochondria of human NP cells, not in agreement with the predominant location of PrPC on the cell surface. However, several recent studies showed that defined populations of neurons express PrPC in the cytoplasm as well as on the plasma membrane (27, 30). PrPC interacts with the C-terminus of Bcl-2 in the mitochondrial transmembrane region (31), and transgenic mice overexpressing wild-type PrPC show the expression of PrPC in the mitochondria (32), suggesting that the mitochondrial location of PrPC in cultured human NP cells does not seem unlikely. Increasing evidence suggests that the conformational conversion of α-helix-rich PrPC into β-sheet-rich PrPSc involves a molecular chaperone-like factor. A previous study using a yeast 2-hybrid system showed that Hsp60 interacts with PrPC, where the docking site was mapped between amino acid residues 180 and 210 of PrPC (33). GroEL, a homolog of eukaryotic Hsp60, mediates the aggregation of recombinant PrPC and promotes the conversion of PrPC into PrPSc in an ATP-dependent manner (23, 24). Furthermore, Hsp60 of the *Brucella abortus* directly binds PrPC of the host macrophages, and this binding promotes the aggregation of PrPC on the cell-surface lipid rafts (34). Interestingly, circulating antibodies against *Spiroplasma* Hsp60 were detected exclusively in patients with CJD, suggesting that the bacterial Hsp60, highly homologous to the host Hsp60, might play an active role in the pathologic process of prion diseases (35). Heat shock elements were identified in the promoter region of prion protein gene (36). PrPC exhibits an antioxidant activity (37), and stress-inducing stimuli such as reactive oxygen species, heat shock, and proinflammatory cytokines elevate the levels of PrPC expression in cultured cells (36, 38, 39). These observations suggest that PrPC and endogenous cellular Hsp are coordinately upregulated in certain cell types under pathologic conditions.

Supporting the present observations, several recent studies identified Hsp60 as one of 14-3-3-interacting proteins in HeLa and HEK293 cells by immunoaffinity purification (9, 40, 41). Hsp60 constitutes a heptameric cylindrical complex composed of identical subunits stacked back to back, forming a double-ring structure. The Anfinsen cage of Hsp60 contains a central cavity where substrate proteins are sequestered and properly folded in cooperation with the Hsp10 family protein (19, 20). In addition, several proteins that are too large to fit the cage are processed for chaperoning outside the cage (42). Hsp60 is located primarily in the mitochondrial matrix, where it mediates the folding of newly imported mitochondrial matrix proteins and the assembly of large multiprotein complexes (43). Importantly, the 14-3-3 protein that does not have a mitochondrial targeting signal is also identified within the mitochondria (44). A recent study showed that an exposure to cisplatin upregulates simultaneously Hsp60 and 14-3-3 expression in human squamous cell carcinoma (45). Kinase suppressor of Ras (KSR), a regulator of the Ras-MAP kinase pathway, forms a multimolecular signaling complex composed of Hsp90, Hsp70, Hsp68, $p50^{CDC37}$, MEK1, MEK2, and 14-3-3 proteins, where a panel of Hsp serve to stabilize KSR (46). It is worthy to note that the levels of expression of the cytosolic chaperonin CCT6A are reduced in the brain of 14-3-3γ isoform-knockout mice, although these mice show a clinical course similar to the wild-type mice after inoculation of scrapie prion (47). Because the 14-3-3 protein acts as an allosteric regulator that stabilizes the binding partners in a particular conformation (3, 4), we could suggest the following scenario (Fig. 9). The interaction of 14-3-3 with PrPC might prevent PrPC from the autocatalytic conformational change under physiological conditions. When affected with the pathogenetic prion, PrPSc aggregates displace 14-3-3

protein from the molecular complex during the conversion of PrPC into PrPSc that is promoted by Hsp60, resulting in the release of 14-3-3 from degenerating neurons into the CSF.

ACKNOWLEDGMENTS

The authors thank Dr. Masashi Fukuda, Invitrogen Proteome, Yokohama, Japan, for his help in nanoESI-MS/MS analysis; and Ms. Chizuru Soma and Ms. Ayako Sakamoto, NCNP, Tokyo, Japan, for their technical assistance. All autopsied brain samples were obtained from the Research Resource Network (RRN), Japan.

REFERENCES

1. Fu H, Subramanian RR, Masters SC. 14-3-3 proteins: Structure, function, and regulation. Annu Rev Pharmacol Toxicol 2000;40:617–47
2. van Hemert MJ, Steensma HY, van Heusden GPH. 14-3-3 proteins: Key regulators of cell division, signaling and apoptosis. Bioessays 2001; 23:936–47
3. Dougherty MK, Morrison DK. Unlocking the code of 14-3-3. J Cell Sci 2004;117:1875–84
4. MacKintosh C. Dynamic interactions between 14-3-3 proteins and phosphoproteins regulate diverse cellular processes. Biochem J 2004;381: 329–42
5. Berg D, Holzmann C, Riess O. 14-3-3 proteins in the nervous system. Nature Rev Neurosci 2002;4:752–62
6. Ostrerova N, Petrucelli L, Farrer M, et al. α-Synuclein shares physical and functional homology with 14-3-3 proteins. J Neurosci 1999;19:5782–91
7. Agarwal-Mawal A, Qureshi HY, Cafferty PW, et al. 14-3-3 connects glycogen synthase kinase-3β to tau within a brain microtubule-associated tau phosphorylation complex. J Biol Chem 2003;278:12722–28
8. Chen H-K, Fernandez-Funez P, Acevedo SF, et al. Interaction of Akt-phosphorylated ataxin-1 with 14-3-3 mediates neurodegeneration in spinocerebellar ataxia type 1. Cell 2003;113:457–68
9. Meek SEM, Lane WS, Piwnica-Worms H. Comprehensive proteomic analysis of interphase and mitotic 14-3-3-binding proteins. J Biol Chem 2004;279:32046–46
10. Zhai J, Lin H, Shamim M, et al. Identification of a novel interaction of 14-3-3 with p190RhoGEF. J Biol Chem 2001;276:41318–24
11. Henriksson ML, Francis MS, Peden A, et al. A nonphosphorylated 14-3-3 binding motif on exoenzyme S that is functional in vivo. Eur J Biochem 2002;269:4921–29
12. Dai J-G, Murakami K. Constitutively and autonomously active protein kinase C associated with 14-3-3 ζ in the rodent brain. J Neurochem 2003;84:23–34
13. Yuan H, Michelsen K, Schwappach B. 14-3-3 dimers probe the assembly status of multimeric membrane proteins. Curr Biol 2003;13:638–46
14. Hsich G, Kenney K, Gibbs CJ Jr., et al. The 14-3-3 brain protein in cerebrospinal fluid as a marker for transmissible spongiform encephalopathies. N Engl J Med 1996;335:924–30
15. Zerr I, Bodemer M, Gefeller O, et al. Detection of 14-3-3 protein in the cerebrospinal fluid supports the diagnosis of Creutzfeldt-Jakob disease. Ann Neurol 1998;43:32–40
16. Richard M, Biacabe A-G, Streichenberger N, et al. Immunohistochemical localization of 14.3.3 ζ protein in amyloid plaques in human spongiform encephalopathies. Acta Neuropathol 2003;105:296–302
17. Prusiner SB. Prions. Proc Natl Acad Sci U S A 1998;95:13363–83
18. Hartl FU, Mayer-Hartl M. Molecular chaperones in the cytosol: From nascent chain to folded protein. Science 2002;295:1852–58
19. Bukau B, Horwich AL. The Hsp70 and Hsp60 chaperone machines. Cell 1998;92:351–66
20. Richardson A, Landry SJ, Georgopoulos C. The ins and outs of a molecular chaperone machine. Trends Biochem Sci 1998;23:138–43
21. Muchowski PJ, Wacker JL. Modulation of neurodegeneration by molecular chaperones. Nature Rev Neurosci 2005;6:11–22
22. Hansen JJ, Dürr A, Cournu-Rebeix I, et al. Hereditary spastic paraplegia SPG13 is associated with a mutation in the gene encoding the mitochondrial chaperonin Hsp60. Am J Hum Genet 2002;70:1328–32
23. DebBurman SK, Raymond GJ, Caughey B, et al. Chaperone-supervised conversion of prion protein to its protease-resistant form. Proc Natl Acad Sci U S A 1997;94:13938–43
24. Stöckel J, Hartl FU. Chaperonin-mediated de novo generation of prion protein aggregates. J Mol Biol 2001;313:861–72
25. Satoh J-I, Kuroda Y. Differential gene expression between human neurons and neuronal progenitor cells in culture: An analysis of arrayed cDNA clones in NTera2 human embryonal carcinoma cell line as a model system. J Neurosci Methods 2000;94:155–64
26. Satoh J-I, Yamamura T, Arima K. The 14-3-3 protein ε isoform expressed in reactive astrocytes in demyelinating lesions of multiple sclerosis binds to vimentin and glial fibrillary acidic protein in cultured human astrocytes. Am J Pathol 2004;165:577–92
27. Kovacs GG, Voigtländer T, Hainfellner JA, et al. Distribution of intraneuronal immunoreactivity for the prion protein in human prion diseases. Acta Neuropathol 2002;104:320–26
28. Bendheim PE, Brown HR, Rudelli RD, et al. Nearly ubiquitous tissue distribution of the scrapie agent precursor protein. Neurology 1992;42: 149–56
29. Moser M, Colello RJ, Pott U, et al. Developmental expression of the prion protein gene in glial cells. Neuron 1995;14:509–17
30. Mironov A Jr, Latawiec D, Wille H, et al. Cytosolic prion protein in neurons. J Neurosci 2003;23:7183–93
31. Kurschner C, Morgan JI. Analysis of interaction sites in homo-and heteromeric complexes containing Bcl-2 family members and the cellular prion protein. Mol Brain Res 1996;37:249–58
32. Hachiya NS, Yamada M, Watanabe K, et al. Mitochondrial localization of cellular prion protein (PrP^C) invokes neuronal apoptosis in aged transgenic mice overexpressing PrP^C. Neurosci Lett 2005;374:98–103
33. Edenhofer F, Rieger R, Famulok M, et al. Prion protein PrP^C interacts with molecular chaperones of the Hsp60 family. J Virol 1996;70: 4724–28
34. Watarai M, Kim S, Erdenebaatar J, et al. Cellular prion protein promotes *Brucella* infection into macrophages. J Exp Med 2003;198:5–17
35. Moyer P. Spiroplasma Hsp60 may be the pathogen responsible for spreading CJD. Neurol Today 2004;4:8–11
36. Shyu W-C, Harn H-J, Saeki K, et al. Molecular modulation of expression of prion protein by heat shock. Mol Neurobiol 2002;26:1–12
37. White AR, Collins SJ, Maher F, et al. Prion protein-deficient neurons reveal lower glutathione reductase activity and increased susceptibility to hydrogen peroxide toxicity. Am J Pathol 1999;155:1723–30
38. Satoh J-I, Kurohara K, Yukitake M, et al. Constitutive and cytokine-inducible expression of prion protein gene in human neural cell lines. J Neuropathol Exp Neurol 1998;57:131–39
39. Sauer H, Dagdanova A, Hescheler J, et al. Redox-regulation of intrinsic prion expression in multicellular prostate tumor sheroids. Free Radic Biol Med 1999;27:1276–83
40. Jin J, Smith FD, Stark C, et al. Proteomic, functional, and domain-based analysis of in vivo 14-3-3 binding proteins involved in cytoskeletal regulation and cellular organization. Curr Biol 2004;14: 1436–50
41. Pozuelo Rubio M, Geraghty KM, Wong BHC, et al. 14-3-3-affinity purification of over 200 human phosphoproteins reveals new links to regulation of cellular metabolism, proliferation and trafficking. Biochem J 2004;379:395–408
42. Chaudhuri TK, Farr GW, Fenton WA, et al. GroEL/GroES-mediated folding of a protein too large to be encapsulated. Cell 2001;107:235–46
43. Cheng MY, Hartl FU, Martin J, et al. Mitochondrial heat-shock protein hsp60 is essential for assembly of proteins imported into yeast mitochondria. Nature 1989;337:620–25
44. Pierrat B, Ito M, Hinz W, et al. Uncoupling proteins 2 and 3 interact with members of the 14.3.3 family. Eur J Biochem 2000;267:2680–87
45. Castagna A, Antonioli P, Astner H, et al. A proteomic approach to cisplatin resistance in the cervix squamous cell carcinoma cell line A431. Proteomics 2004;4:3246–67
46. Stewart S, Sundaram M, Zhang Y, et al. Kinase suppressor of Ras forms a multiprotein signaling complex and modulates MEK localization. Mol Cell Biol 1999;19:5523–34
47. Steinacker P, Schwarz P, Reim K, et al. Unchanged survival rates of 14-3-3γ knockout mice after inoculation with pathological prion protein. Mol Cell Biol 2005;25:1339–46

Modulation of CD1d-restricted NKT cell responses by using *N*-acyl variants of α-galactosylceramides

Karl O. A. Yu*†, Jin S. Im*†, Alberto Molano*†, Yves Dutronc*‡, Petr A. Illarionov§, Claire Forestier*, Nagatoshi Fujiwara*¶, Isa Arias*, Sachiko Miyake‖, Takashi Yamamura‖, Young-Tae Chang**, Gurdyal S. Besra§, and Steven A. Porcelli*††

*Department of Microbiology and Immunology, Albert Einstein College of Medicine, 1300 Morris Park Avenue, Bronx, NY 10461; §School of Biosciences, University of Birmingham, Edgbaston, Birmingham B15 2TT, United Kingdom; ‖Department of Immunology, National Institute of Neuroscience, National Center of Neurology and Psychiatry, 4-1-1 Ogawahigashi, Kodaira, Tokyo 187-8502, Japan; and **Department of Chemistry, New York University, 29 Washington Place, New York, NY 10003

Edited by Douglas T. Fearon, University of Cambridge, Cambridge, United Kingdom, and approved January 18, 2005 (received for review October 8, 2004)

A form of α-galactosylceramide, KRN7000, activates CD1d-restricted Vα14-invariant (Vα14i) natural killer (NK) T cells and initiates multiple downstream immune reactions. We report that substituting the C26:0 *N*-acyl chain of KRN7000 with shorter, unsaturated fatty acids modifies the outcome of Vα14i NKT cell activation. One analogue containing a diunsaturated C20 fatty acid (C20:2) potently induced a T helper type 2-biased cytokine response, with diminished IFN-γ production and reduced Vα14i NKT cell expansion. C20:2 also exhibited less stringent requirements for loading onto CD1d than KRN7000, suggesting a mechanism for the immunomodulatory properties of this lipid. The differential cellular response elicited by this class of Vα14i NKT cell agonists may prove to be useful in immunotherapeutic applications.

cytokines | inflammation | autoimmunity | immunoregulation

Natural killer (NK) T cells were defined originally as lymphocytes coexpressing T cell receptors (TCRs) and C-type lectin receptors characteristic of NK cells. A major subset of NKT cells recognizes the MHC class I-like molecule CD1d by using TCRs composed of an invariant TCR-α chain (mouse Vα14-Jα18, human Vα24-Jα18) paired with TCR-β chains with markedly skewed Vβ usage (1). These CD1d-restricted Vα14-invariant (Vα14i) NKT cells are highly conserved in phenotype and function between mice and humans (2). Vα14i NKT cells influence various immune responses and play an important role in regulating autoimmunity (3, 4). One example is the nonobese diabetic mouse. When compared with normal mice, nonobese diabetic mice have fewer Vα14i NKT cells, which are defective in their capacity to produce antiinflammatory cytokines like IL-4 (5, 6). Deficiencies in NKT cells have also been observed in humans with various autoimmune diseases (7, 8).

Vα14i NKT cells have been manipulated to prevent or treat autoimmune disease, mostly through the use of KRN7000, a synthetic α-galactosylceramide (α-GalCer, Fig. 1*A*) that binds to the hydrophobic groove of CD1d and then activates Vα14i NKT cells by means of TCR recognition (9). KRN7000 treatment of nonobese diabetic mice blocks development of T helper (T_H) type 1-mediated autoimmune destruction of pancreatic islet β-cells, thus delaying or preventing disease (10–12). There has been considerable interest in methods that would allow a more selective activation of these cells. In particular, the ability to trigger IL-4 production without eliciting strong IFN-γ or other proinflammatory cytokines may reinforce the immunoregulatory functions of Vα14i NKT cells. This effect is detected after Vα14i NKT cell activation with a glycolipid designated OCH, which is an α-GalCer analogue that is structurally distinct from KRN7000 in having a substantially shorter sphingosine chain and functionally by its preferential induction of IL-4 secretion (13, 14).

In this study, we investigated responses to α-GalCer analogues produced by alteration of the length and extent of unsaturation of their *N*-acyl substituents. Such modifications altered the outcome of Vα14i NKT cell activation and, in some cases, led to a T_H2-biased and potentially antiinflammatory cytokine response. This change in the NKT cell response was likely the result of an alteration of downstream steps in the cascade of events triggered by Vα14i NKT cell activation, including the reduction of secondary activation of IFN-γ-producing NK cells. These findings point to a class of Vα14i NKT cell agonists that may have superior properties for the treatment of autoimmune and inflammatory diseases.

Materials and Methods

Mice and Cell Lines. C57BL/6 mice (8- to 15-wk-old females) were obtained either from The Jackson Laboratory or Taconic Farms. $CD1d^{-/-}$ mice were provided by M. Exley and S. Balk (Beth Israel–Deaconess Medical Center, Harvard Medical School, Boston) (15). Vα14i NKT cell-deficient $J\alpha18^{-/-}$ mice were a gift from M. Taniguchi and T. Nakayama (Chiba University, Chiba, Japan) (16). Both knockout mice were in the C57BL/6 background. Animals were kept in specific pathogen-free housing. The protocols that we used were in accordance with approved institutional guidelines.

Mouse CD1d-transfected RMA-S cells (RMA-S.mCD1d) were provided by S. Behar (Brigham and Women's Hospital, Harvard Medical School) (17). WT or cytoplasmic tail-deleted CD1d-transfected A20 cells and the Vα14i NKT hybridoma DN3A4–1.2 were provided by M. Kronenberg (La Jolla Institute for Allergy and Immunology, La Jolla, CA) (18, 19). Hybridoma DN32D3 was a gift from A. Bendelac (University of Chicago, Chicago) (1). Cells were cultured in RPMI medium 1640 (GIBCO) supplemented with 10% heat-inactivated FCS (Gemini Biological Products, Calabasas, CA)/10 mM Hepes/2 mM L-glutamine/0.1 mM nonessential amino acids/55 μM 2-mercaptoethanol/100 units/ml penicillin/100 μg/ml streptomycin (GIBCO) in a 37°C humidified incubator with 5% CO_2.

Glycolipids. BF1508-84 was synthesized by Biomira (Edmonton, Canada). OCH [(2*S*, 3*S*, 4*R*)-1-*O*-(α-D-galactopyranosyl)-*N*-tetracosanoyl-2 amino-1,3,4-nonanetriol] was synthesized as described (13). An overview of the methods for synthesis of KRN7000 [(2*S*, 3*S*, 4*R*)-1-*O*-(α-D-galactopyranosyl)-*N*-hexaco-

This paper was submitted directly (Track II) to the PNAS office.

Abbreviations: Vα14i, Vα14 invariant; NK, natural killer; α GalCer, α galactosylceramide; T_H, T helper; TCR, T cell receptor; RMA S.mCD1d, mouse CD1d transfected RMA S cells.

†K.O.A.Y., J.S.I., and A.M. contributed equally to this work.

‡Present address: Department of Dermatology, Bocage Hospital, BP 77908, 21079 Dijon Cedex, France.

¶Present address: Department of Host Defense, Graduate School of Medicine, Osaka City University, 1-4-3 Asahi-machi, Abeno-ku, Osaka 545-8585, Japan.

††To whom correspondence should be addressed. E-mail: porcelli@aecom.yu.edu.

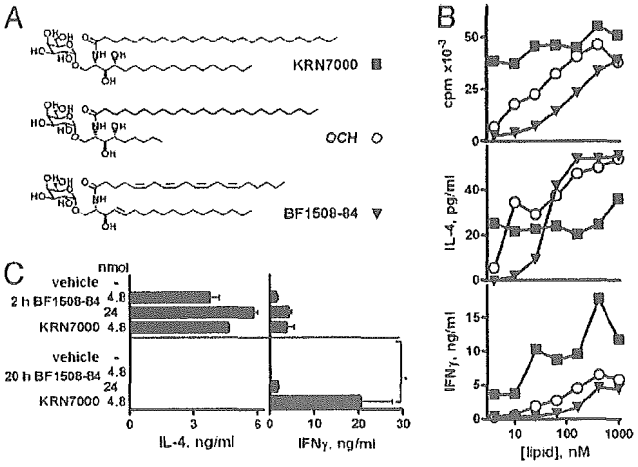

Fig. 1. Induction of a T_H2-polarized cytokine response by an unsaturated analogue of α-GalCer. (*A*) Glycolipid structures. (*B*) [^{3}H]thymidine incorporation and supernatant IL-4 and IFN-γ levels in 72-h splenocyte cultures with graded amounts of glycolipid. Means from triplicate cultures are shown; SEMs were typically <10% of the mean. (*C*) Serum IL-4 and IFN-γ levels (at 2 and 20 h) of C57BL/6 mice injected i.p. with 4.8 or 24 nmol of glycolipid. KRN7000 was the only glycolipid that induced significant IFN-γ levels at 20 h (*, $P < 0.05$, Kruskall–Wallis test, Dunn's posttest). Means ± SD of two or three mice per group are shown.

sanoyl-2-amino-1,3,4-octadecanetriol] and other *N*-acyl analogues used in this study is shown in Fig. 7, which is published as supporting information on the PNAS web site. Lipids were dissolved in chloroform/methanol (2:1 ratio) and stored at −20°C. Aliquots from this stock were dried and reconstituted to either 100 μM in DMSO for *in vitro* work or to 500 μM in 0.5% Tween-20 in PBS for *in vivo* studies.

***In Vitro* Stimulations.** Bulk splenocytes were plated at 300,000 cells per well in 96-well flat-bottom tissue culture plates with glycolipid diluted in 200 μl of medium. After 48 or 72 h at 37°C, 150 μl of supernatant was removed for cytokine measurements, and 0.5 μCi (1 Ci = 37 GBq) [^{3}H]thymidine per well (specific activity 2 Ci/mmol; PerkinElmer) was added for an 18-h pulse. Proliferation was estimated by harvesting cells onto 96-well filter mats and counting β-scintillations with a 1450 Microbeta Trilux (Wallac, Gaithersburg, MD; PerkinElmer).

Supernatant levels of IL-2, IL-4, IL-12p70, and IFN-γ were measured by ELISA using capture and biotinylated detection antibody pairs (BD PharMingen) and streptavidin–horseradish peroxidase (Zymed) with TMB-Turbo substrate (Pierce) or streptavidin–alkaline phosphatase (Zymed) with 4-nitrophenyl phosphate substrate (Sigma). IL-2 standard was obtained from R & D Systems; IL-4, IL-12p70, and IFN-γ were obtained from PeproTech (Rocky Hill, NJ).

Hybridoma Stimulations. CD1d$^+$ RMA-S or A20 cells (50,000 cells in 100 μl per well) were pulsed with graded doses of glycolipid for 6 h at 37°C. After three washes in PBS, Vα14i NKT hybridoma cells (50,000 cells in 100 μl) were added for 12 h. Supernatant IL-2 was assayed by ELISA. Alternatively, CD1d-transfected cells (RMA-S.mCD1d) were lightly fixed either before or after exposure to antigen (20). Cells were washed twice in PBS and then fixed in 0.05% glutaraldehyde (grade I, Sigma) in PBS for 30 s at room temperature. Fixative was quenched by addition of 0.2 M L-lysine (pH 7.4) for 2 min, followed by two washes with medium before addition of responders.

For cell-free presentation, recombinant mouse CD1d (1 μg/ml in PBS) purified from a baculovirus expression system (21) was adhered to tissue culture plates for 1 h at 37°C. After the washing off of unbound protein, glycolipids were then added at varying concentrations for 1 h at 37°C. Lipids were added in a 150 mM NaCl/10 mM sodium phosphate buffer (pH 7) with or without 0.025% Triton X-100. Wells were washed before addition of hybridoma cells.

***In Vivo* Studies.** Mice were given i.p. injections of 4.8 nmol of glycolipid in 0.2 ml of PBS plus 0.025% Tween-20 or vehicle alone. Sera were collected and tested for IL-4, IL-12p70, and IFN-γ, as described above. Alternatively, mice were killed at various times for FACS analysis.

Flow Cytometry. Splenocytes or thymocytes were isolated and used without further purification. Nonspecific staining was blocked by using FACS buffer (0.1% BSA/0.05% NaN_3 in PBS) with 10 μg/ml rat anti-mouse CD16/32 (2.4G2; The American Type Culture Collection). Cells ($\leq 10^6$) were stained with phycoerythrin or allophycocyanin-conjugated glycolipid/mouse CD1d tetramers (21) for 30–90 min at room temperature and then with fluorescently labeled antibodies (from Caltag, South San Francisco, CA, or PharMingen) for 30 min at 4°C. Data were acquired on either a FACSCalibur or LSR-II flow cytometer (Becton Dickenson) and analyzed by using WINMDI 2.8 (Scripps Research Institute, La Jolla, CA). For some experiments, dead cells were excluded by using propidium iodide (Sigma) or 4′,6-diamidino-2-phenylindole (Roche).

FACS-based cytokine secretion assays (Miltenyi Biotec, Auburn, CA) were used to quantitatively detect single-cell production of IL-4 or IFN-γ. Splenocytes were aseptically collected from mice that were previously injected i.p. with glycolipid analogues and not subjected to further stimulation. When applicable, 10^6 cells were prestained with labeled tetramer for 30 min at room temperature and then washed in PBS plus 0.1% BSA. Cells were then stained with the cytokine catch reagent according to the manufacturer's instructions, followed by incubation with rotation in 2 ml of medium at 37°C for 45 min. Cells were then washed, stained with fluorescently labeled antibodies to cell-surface antigens, phycoerythrin-conjugated anti-IFN-γ or IL-4, and propidium iodide, as described above.

Results

T_H2-Skewing Properties of an α-GalCer Analogue. During screening of a panel of synthetic glycosyl ceramides, we identified a compound that showed T_H2-skewing of the cytokine profile generated by Vα14i NKT cell activation. Glycolipid BF1508-84 differed structurally from both OCH and KRN7000 by having a shortened, unsaturated fatty-acid chain (C20:4 arachidonate) and a double bond in place of the 4-hydroxy in the sphingosine base (Fig. 1*A*). Despite these modifications, BF1508-84 activated proliferation and cytokine secretion by mouse splenocytes (Fig. 1*B*). These responses were Vα14i NKT cell-dependent, as demonstrated by their absence in both CD1d$^{-/-}$ and Jα18$^{-/-}$ mice (data not shown). Maximal proliferation and IL-4 levels were comparable with those obtained with KRN7000 and OCH, although a higher concentration of BF1508-84 was required to reach similar responses. Interestingly, IFN-γ secretion stimulated by BF1508-84, even at higher tested concentrations, did not reach the levels seen with KRN7000. This profile of cytokine responses suggested that BF1508-84 can elicit a T_H2-biased Vα14i NKT cell-dependent cytokine production, similar to OCH (13).

We measured serum cytokine levels at various times after a single injection of either KRN7000 or BF1508-84 into C57BL/6 mice. Our studies confirm published reports that a single i.p. injection of KRN7000 leads to a rapid 2-h peak of serum IL-4 (Fig. 1*C* and data not shown). However, IFN-γ levels were relatively low at 2 h but rose to a plateau at 12–24 h (13, 22). With

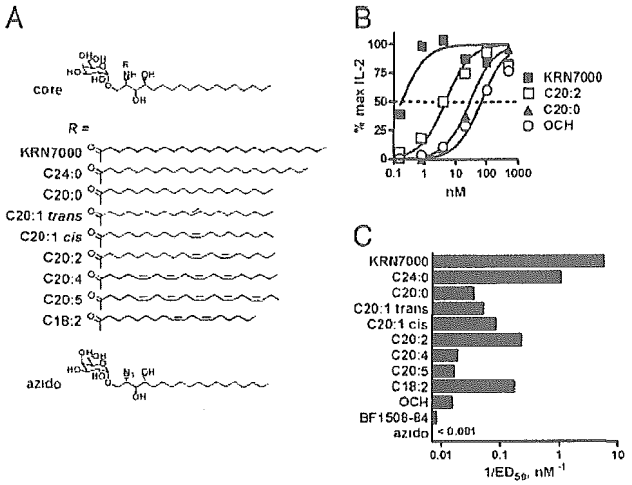

Fig. 2. Recognition of a panel of unsaturated analogues of KRN7000 by a canonical Vα14i NKT hybridoma. (*A*) Analogue structures. (*B*) Dose–response curves showing IL-2 production by hybridoma DN3A4–1.2 after stimulation with RMA-S.mCD1d cells pulsed with various doses of glycolipid. Maximal IL-2 concentrations in each assay were designated as 100%. Four-parameter logistic equation dose–response curves are shown; the dotted line denotes the half-maximal dose. (*C*) Relative potencies of the analogue panel in Vα14i NKT cell recognition, plotted as the reciprocal of the effective dose required to elicit a half-maximal response ($1/ED_{50}$). Similar results were obtained by using another Vα14i NKT hybridoma, DN32D3.

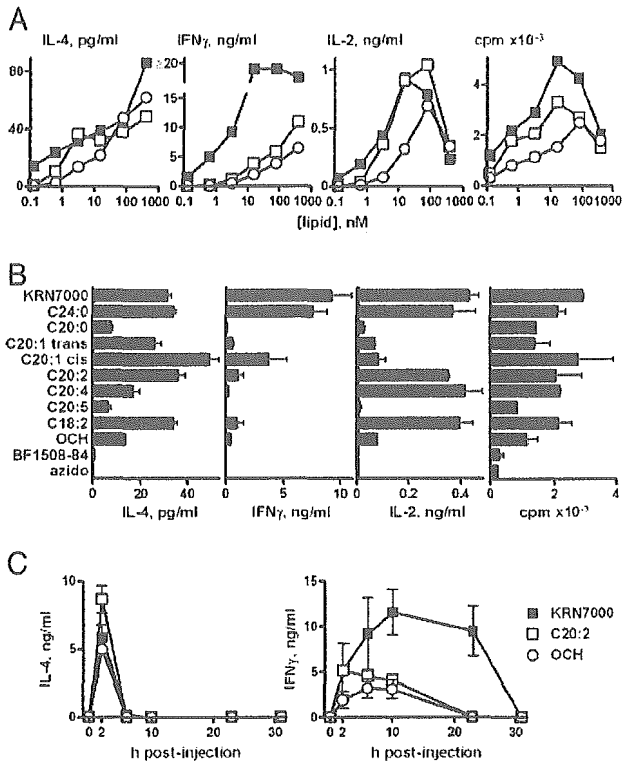

Fig. 3. T_H2-skewing of *in vitro* and *in vivo* cytokine responses to C20:2. (*A*) Dose–response curves reporting 48 h IL-4, IFN-γ, or IL-2 production, and cell proliferation of splenocytes in response to KRN7000, C20:2, and OCH. Means of duplicate cultures are shown; SEM were < 10% of the means. (*B*) Cytokine and proliferation measurements on splenocytes exposed to a submaximal dose (3.2 nM) of the panel of α-GalCer analogues shown in Fig. 2. Mean ± SEM from duplicate cultures shown. (*C*) Serum IL-4 and IFN-γ levels in mice given 4.8 nmol of KRN7000, C20:2, or OCH. Mean ± SD of two or three mice are shown. Vehicle-treated mice had cytokine levels below limits of detection. The results shown are representative of two or more experiments.

BF1508-84, production of IL-4 at 2 h was preserved, whereas IFN-γ was barely detectable at 20 h (Fig. 1*C*). This pattern was identical to that reported for OCH (13, 22) and was not due to the lower potency of BF1508-84 because a 5-fold greater dose did not change the T_H2-biased cytokine profile (Fig. 1*C*).

Systematic Variation of Fatty-Acyl Unsaturation in α-GalCer. The cytokine response to BF1508-84 suggested that altering the fatty-acid length and unsaturation of α-GalCer could provide an effective strategy for creating Vα14i NKT cell activators with modified functional properties. We used a synthetic approach (Fig. 7, and G.S.B. and P.A.I., unpublished data) to generate lipids in which 20-carbon acyl chains with varying degrees of unsaturation were coupled onto the α-galactosylated sphingosine core structure (Fig. 2*A*). These compounds were first screened for the ability to activate a canonical Vα14-Jα18/Vβ8.2$^+$, CD1d-restricted NKT cell hybridoma cocultured with CD1d$^+$ antigen-presenting cells. Hybridoma DN3A4–1.2 recognized all C20 analogues of α-GalCer with various potencies when presented by CD1d-transfected RMA-S cells, and it failed to recognize an azido-substituted analogue lacking a fatty-acid chain (Fig. 2 *B* and *C*). As reported (9), mere shortening of the fatty-acid chain affected Vα14i NKT cell recognition, and reduction of saturated fatty-acid length from C26 to C20 was associated with a ≈2 log decrease in potency. However, insertion of double bonds into the C20 acyl chain augmented stimulatory activity. One lipid in particular, with unsaturations at carbons 11 and 14 (C20:2), was more potent than other analogues in the panel. This increase in potency seemed to be a direct result of the two double bonds, because an independently synthesized analogue with a slightly shorter diunsaturated acyl chain (C18:2) showed a potency similar to that of C20:2 (Fig. 2*C*).

We also studied *in vitro* splenocyte cytokine polarization resulting from Vα14i NKT cell stimulation by each lipid in the panel. Supernatant IL-4, IFN-γ, and IL-2 levels were measured over a wide range of glycolipid concentrations. All C20 variants induced IL-4 production comparable with that of KRN7000 (Fig. 3*A* and *B*, and data not shown). However, IFN-γ levels for all but one C20 analogue (C20:1 *cis*) were markedly reduced to one-fourth of the maximal levels observed with KRN7000 and the closely related C24:0 analogue, or less. In addition, C20:1-*cis*, C20:2, and C18:2 were unique in this class of compounds in inducing strong IL-2 production and cellular proliferation similar to that seen with KRN7000 and C24:0 yet with much lower IFN-γ induction. This *in vitro* T_H2-bias was also evident *in vivo*. Mice given C20:2 and C20:4 showed systemic cytokine production that resembled stimulation by OCH or BF1508-84. Thus, a rapid burst of serum IL-4 was observed without the delayed and sustained production of IFN-γ typical of KRN7000 (Fig. 3*C* and data not shown). No significant difference between the glycolipids was seen in serum IL-12p70 levels at 6 h after treatment (data not shown).

Identification of Cytokine-Producing Cells *in Vivo*. Previous reports (23–25) established that Vα14i NKT cells are a predominant source of IL-4 and IFN-γ in the early (2 h) response to KRN7000 and that by 6 h after injection these cells become progressively undetectable because of receptor down-modulation, whereas secondarily activated NK cells begin to actively produce IFN-γ. Gating on either α-GalCer-loaded CD1d tetramer$^+$ or NK1.1$^+$ T cells, we observed similar strong cytokine secretion for both IL-4 (data not shown) and IFN-γ in Vα14i NKT cells at 2 h after injection of KRN7000 or C20:2 (Fig. 4 *A* and *B*). We concluded

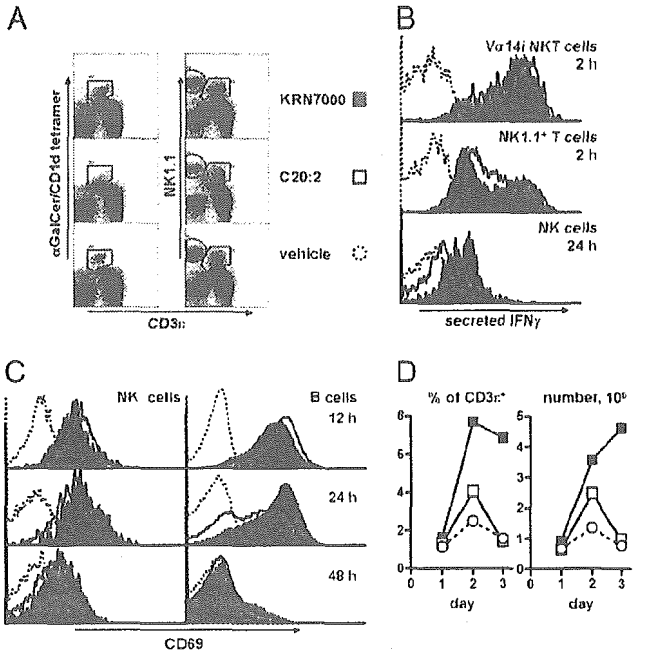

Fig. 4. Sequelae of KRN7000 and C20:2-induced Vα14i NKT cell activation. (*A*) Vα14i NKT cell (tetramer$^+$ CD3ε^{int}), NK cell (NK1.1$^+$ CD3ε^-), and NK1.1$^-$ T cell (NK1.1^{int} CD3ε^{int}) identification by FACS in splenocytes from mice given KRN7000, C20:2, or vehicle i.p. 2 h earlier. Lymphocytes gated as negative for B220 and propidium iodide are shown. (*B*) Histogram profiles for IFN-γ secretion of splenic Vα14i NKT, NK1.1$^+$ T, or NK cells from mice 2 or 24 h after treatment with glycolipid. IFN-γ-staining in C24:0-stimulated samples was identical to that of KRN7000-stimulated samples. (*C*) CD69 levels of splenic NK cells (gated as CD3ε^- NK1.1$^+$) or B cells (CD3ε^- NK1.1$^-$ B220$^+$) at 12, 24, or 48 h after injection of glycolipid. (*D*) Splenic Vα14i NKT cell (B220$^-$ CD3ε^{int} tetramer$^+$) frequency, measured as either percentages of T cells or as total NKT cell number, in mice 1, 2, or 3 days after glycolipid administration. The results shown are representative of three independent experiments.

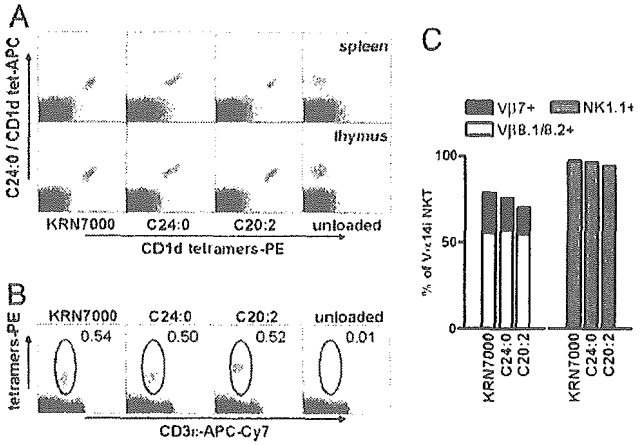

Fig. 5. Recognition of KRN7000, C24:0, and C20:2 by the same population of Vα14i NKT cells. (*A*) Costaining of C57BL 6 splenocytes or thymocytes with allophycocyanin-conjugated CD1d tetramers assembled with C24:0, and phycoerythrin-labeled CD1d tetramers assembled with various analogues. (*B*) Thymocytes were stained with C24:0, C20:2, KRN7000, or vehicle-loaded CD1d tetramers–phycoerythrin, and with antibodies to B220, CD3ε, Vβ7, Vβ8.1 8.2, or NK1.1. Dot plots show gating for tetramer$^+$ T cells, after exclusion of B lymphocytes, and dead cells. (*C*) TCR Vβ and NK1.1 phenotype of tetramer$^+$ CD3ε^{int} thymocytes. Analogous results were obtained with splenocytes. The results shown are representative of three or more experiments.

that cytokine polarization observed after C20:2 administration was not due to differences in the initial Vα14i NKT cell response but, rather, reflected altered downstream events such as the relatively late IFN-γ production by activated NK cells.

Secreted cytokine staining confirmed that in both KRN7000- and C20:2-treated mice, NK cells were IFN-γ$^+$ at 6–12 h after treatment (26, 27). However, whereas splenic NK cells from mice that received either KRN7000 or the closely related C24:0 analogue strongly produced IFN-γ as late as 24 h after initial activation, NK cells from C20:2-treated mice showed substantially reduced staining (Fig. 4*B*). Together, these results pointed to a less sustained secondary IFN-γ production by NK cells (rather than a change in the initial cytokine response of Vα14i NKT cells) as the major factor responsible for the T_H2 bias of the systemic cytokine response to C20:2.

Sequelae of Vα14i NKT Cell Activation by C20:2. Secondary activation of bystander B and NK cells after KRN7000 administration has been studied by using expression of the activation marker CD69 (26, 28–30). We followed CD69 expression of splenic NK and B cell populations for several hours after KRN7000 or C20:2 administration. Both populations began to up-regulate CD69 at 4–6 h after injection (data not shown). Paradoxically, C20:2 induced slightly higher CD69 levels on both cell populations up until 12 h, although this trend was reversed from 24 h onwards, suggesting an earlier up-regulation yet faster subsequent down-regulation of the marker (Fig. 4*C*). NK cell forward scatter likewise remained higher in KRN7000-treated mice at days 1–3 compared with C20:2-treated mice (data not shown).

It is established that Vα14i NKT cells expand beyond homeostatic levels 2 or 3 days after KRN7000 stimulation (24, 25). In our study, a 3- to 5-fold expansion in splenic Vα14i NKT cell number occurred in KRN7000-treated mice at day 3 after injection. Interestingly, after *in vivo* administration of C20:2, only a minimal transient expansion was observed on day 2, with no expansion of the Vα14i NKT cell population thereafter, even as late as day 5 (Fig. 4*D* and data not shown). Together, our findings indicated pronounced alterations in the late sequelae of Vα14i NKT cell activation with the C20:2 analogue compared with KRN7000.

Recognition of KRN7000 and C20:2 by Identical Cell Populations. CD1d complexes containing the α-GalCer analogue OCH have been shown to have significantly reduced avidity for TCRs of Vα14i NKT cells compared with binding of KRN7000-loaded complexes (31). This finding suggests the possibility that the T_H2-biased response of C20:2 could be a result of preferential stimulation of Vα14i NKT cell subsets with TCRs of higher affinity for lipid-loaded CD1d. In fact, phenotypically defined subsets of murine and human NKT cells have been described that show a bias toward increased production of IL-4 relative to IFN-γ upon stimulation (32–36). However, by costaining of splenic and thymic Vα14i NKT cells by using CD1d tetramers loaded with different lipids, we demonstrated that identical populations recognized C24:0, C20:2, and KRN7000 (Fig. 5*A*). Single staining with these reagents revealed no difference in Vβ usage or NK1.1 status of cells reactive with the different analogue tetramers (Fig. 5 *B* and *C*). Interestingly, C20:2-loaded tetramers stained NKT cells more strongly than tetramers loaded with KRN7000, reflecting a slightly higher affinity of the C20:2–CD1d complex to the Vα14i TCR (J.S.I. and S.A.P., unpublished results). Together, these findings demonstrated that the altered cytokine response to C20:2 cannot be the result of preferential activation of a subset of Vα14i NKT cells.

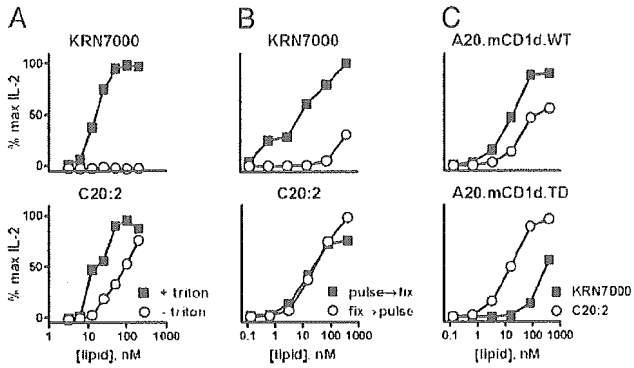

Fig. 6. Differential requirements for CD1d loading with KRN7000 and C20:2. IL-2 response of hybridoma DN3A4–1.2 to glycolipid presentation in three *in vitro* CD1d presentation systems: platebound CD1d loaded with varying amounts of KRN7000 or C20:2 in the presence or absence of the detergent Triton X-100 (*A*), RMA-S.CD1d cells pulsed with glycolipid before or after glutaraldehyde fixation (*B*), or WT or cytoplasmic tail-deleted (TD) CD1d-transfected A20 cells, loaded with either KRN7000 or C20:2 (*C*).

Loading Requirements of α-GalCer Analogues onto CD1d. To find an alternative explanation for the T_H2-biased response to C20:2, we studied requirements for handling of different forms of α-GalCer by antigen-presenting cells. We employed a cell-free system in which platebound mouse CD1d was loaded with doses of KRN7000 or C20:2 in the presence or absence of the detergent Triton X-100 (37). By using IL-2 production by DN3A4–1.2 as a readout for glycolipid loading of CD1d, we observed a marked dependence on detergent for loading of KRN7000 but not for C20:2 (Fig. 6*A*). This result suggested a significant difference in requirement for cofactors, such as acidic pH or lipid transfer proteins, that facilitate lipid loading onto CD1d in endosomes (38–41). We assessed this hypothesis further by using glutaraldehyde fixation of $CD1d^+$ antigen-presenting cells, which blocks antigen uptake and recycling of CD1d between endosomes and the plasma membrane. Vα14i NKT cell recognition of KRN7000 was markedly reduced if lipid loading was done after fixation of RMA-S.mCD1d cells, whereas recognition of C20:2 was unimpaired (Fig. 6*B*).

Similar conclusions were drawn from experiments by using A20 cells transfected with either WT or cytoplasmic tail-deleted CD1d (Fig. 6*C*). The tail-deleted CD1d mutant lacks the intracellular tyrosine-based sorting motif required for internalization and endosomal localization of CD1d (19). As was the case with RMA-S.mCD1d, WT CD1d-transfected A20 cells presented KRN7000 more potently than C20:2. However, the tail-deleted mutant presented C20:2 with at least 20-fold greater efficiency than KRN7000. Together, these results point to the conclusion that the T_H2-skewing C20:2 analogue had substantially less dependence on endosomal loading for presentation by CD1d when compared with compounds that produced a more mixed response with strong IFN-γ production, such as KRN7000.

Discussion

This study details *in vitro* and *in vivo* consequences of activation of Vα14i NKT cells with C20:2, a diunsaturated *N*-acyl substituted analogue of the prototypical α-GalCer, KRN7000. The T_H2 cytokine bias observed with C20:2 is not unique: OCH and other shortened fully saturated lipids have been shown to have this effect (13, 42). C20:2 differs from these other compounds in two potentially important respects. First, the *in vitro* potency of C20:2 for stimulation of certain Vα14i NKT cell functions (e.g., proliferation and secretion of IL-4 and IL-2) approaches that of KRN7000, whereas OCH appears to be a much weaker Vα14i NKT cell agonist. Second, staining with C20:2-loaded CD1d tetramers, as opposed to OCH, is undiminished compared with KRN7000. This finding would suggest that, as a therapeutic agent, C20:2 will be recognized by the identical global Vα14i NKT cell population (as KRN7000 is) and not limited to higher-affinity NKT cell subsets, as suggested for OCH (31).

A recent study showed that one mechanism by which OCH may induce a T_H2-biased cytokine response involves changes in IFN-γ production by Vα14i NKT cells themselves. Oki *et al.* (43) reported that the transcription factor gene *c-Rel*, a member of the NF-κB family of transcriptional regulators that is a crucial component of IFN-γ production, is inducibly transcribed in KRN7000-stimulated but not OCH-stimulated Vα14i NKT cells. Although we have not assessed *c-Rel* induction or other factors involved in IFN-γ production in response to C20:2, our findings did not suggest that early IFN-γ production by Vα14i NKT cells was different after activation with C20:2 versus KRN7000. Both lipids induced identical single-cell IFN-γ staining in Vα14i NKT cells and serum IFN-γ levels at 2 h after injection. However, in contrast to the apparent similarity in Vα14i NKT cells, NK cell IFN-γ production was significantly reduced and less sustained after *in vivo* administration of C20:2 compared with KRN7000. Hence, failure of C20:2 to fully activate downstream events leading to optimal NK cell secondary stimulation by activated Vα14i NKT cells appears to be the most likely mechanism by which C20:2 induces reduced IFN-γ and an apparent T_H2-biased systemic response.

C20:2 administration resulted also in a more rapid but less sustained CD69 up-regulation in NK and B cells, as well as a lack of a substantial Vα14i NKT cell expansion. These findings were surprising, given that TCR down-modulation observed on Vα14i NKT cells within the first few hours after C20:2 stimulation was similar to or greater than that induced by KRN7000 (Fig. 4*A* and data not shown), indicating strong TCR signaling in response to the analogue. These features of the response to C20:2 may be a further reflection of the failure of C20:2 to induce a full range of downstream events after Vα14i NKT cell activation, including the production of cytokines or other factors required to support the expansion of Vα14i NKT cells.

What mechanism can then be invoked to account for the altered cytokine response to C20:2 and other *N*-acyl variants of KRN7000? One intriguing possibility is provided by our analysis of requirements for presentation of C20:2 compared with KRN7000, which revealed marked differences between these glycolipids in their need for endosomal loading onto CD1d. CD1d and other CD1 proteins undergo transport into the endocytic pathway, leading to intracellular loading with lipid antigens and subsequent recycling to the cell surface (39). The importance of endosomal loading for KRN7000 most likely reflects the impact of factors in these compartments that facilitate the insertion of lipids into the CD1d ligand-binding groove. These factors include the acidic pH of the endosomal environment, as well as lipid transport proteins, such as saposins and GM2 activator protein (38, 40, 41). Our findings indicate that C20:2 can efficiently load onto CD1d in the absence of these endosomal cofactors. Consequently, we speculate that C20:2 may be strongly presented by any cell type that expresses surface CD1d, regardless of its ability to efficiently endocytose lipids from the extracellular space. This more widespread presentation could lead to a more pronounced presentation of C20:2 by nonprofessional antigen-presenting cell types compared with KRN7000. Because many cell types express CD1d, including all hematopoietic lineages and various types of epithelia (44–48), presentation of C20:2 by nonprofessional antigen-presenting cells may explain the more rapid trans-activation of bystander cells observed with C20:2. An alternative hypothesis is that the endosomal loading requirements of KRN7000 result in its preferential localization into CD1d molecules contained in membrane lipid rafts, whereas the permissive loading properties of

C20:2 would result in a more uniform glycolipid distribution across the cell membrane. Evidence of lipid raft localization of CD1d and raft influence on the T_H-bias of MHC class II-restricted $CD4^+$ T cells lend support to this model (49, 50). Either scenario would be expected to result in decreased delivery of costimulatory signals associated with professional antigen-presenting cells (e.g., dendritic cells) and, thus, lead to quantitative and qualitative differences in the outcome of Vα14i NKT cell stimulation. Consistent with both models, *Vα14i* NKT cell activation with KRN7000 *in vitro* in the presence of costimulatory blockade (anti-CD86) can polarize cytokine production to a T_H2 profile (22).

We have shown that structurally modified forms of α-GalCer with alterations in their *N*-acyl substituents can be designed to generate potent immunomodulators that stimulate qualitatively altered responses from Vα14i NKT cells. Our results confirm and extend several basic observations and principles established from earlier studies on less potent agonists, such as OCH. Further study of these and similar analogues may yield compounds with clear advantages for treatment or prevention of specific immunologic disorders or for the stimulation of protective host immunity against particular pathogens.

We thank R. Koganty and S. Gandhi (Biomira) for sharing their panel of synthetic glycosylceramides, which included compound BF1508-84; M. Kronenberg for the recombinant baculovirus used for production of soluble mouse CD1d; M. Taniguchi, T. Nakayama, A. Bendelac, M. Exley, S. Balk, S. Behar, and M. Kronenberg for gifts of mice and cell lines; Z. Hu for expert technical assistance; and T. DiLorenzo for critical reading of this manuscript. This work was supported by National Institutes of Health Grants AI45889, AI48933, and DK068690 (to S.A.P.), the Japan Human Sciences Foundation (T.Y. and S.A.P.), the Pharmaceutical and Medical Devices Agency (T.Y.), Medical Research Council Grants G9901077 and G0000895 (to G.S.B.), and Wellcome Trust Grants 060750 and 072021 (to G.S.B.). G.S.B. is a Lister Jenner Research Fellow.

1. Lantz, O. & Bendelac, A. (1994) *J. Exp. Med.* **180,** 1097–1106.
2. Brossay, L. & Kronenberg, M. (1999) *Immunogenetics* **50,** 146–151.
3. Godfrey, D. I., Hammond, K. J., Poulton, L. D., Smyth, M. J. & Baxter, A. G. (2000) *Immunol. Today* **21,** 573–583.
4. Wilson, S. B. & Delovitch, T. L. (2003) *Nat. Rev. Immunol.* **3,** 211–222.
5. Poulton, L. D., Smyth, M. J., Hawke, C. G., Silveira, P., Shepherd, D., Naidenko, O. V., Godfrey, D. I. & Baxter, A. G. (2001) *Int. Immunol.* **13,** 887–896.
6. Gombert, J.-M., Tancrede-Bohin, T., Hameg, A., do Carmo Leite-de-Moraes, M., Vicari, A. P., Bach, J.-F. & Herbelin, A. (1996) *Int. Immunol.* **8,** 1751–1758.
7. Van Der Vliet, H. J., Von Blomberg, B. M., Nishi, N., Reijm, M., Voskuyl, A. E., van Bodegraven, A. A., Polman, C. H., Rustemeyer, T., Lips, P., Van Den Eertwegh, A. J., *et al.* (2001) *Clin. Immunol.* **100,** 144–148.
8. Taniguchi, M., Harada, M., Kojo, S., Nakayama, T. & Wakao, H. (2003) *Annu. Rev. Immunol.* **21,** 483–513.
9. Kawano, T., Cui, J., Koezuka, Y., Toura, I., Kaneko, Y., Motoki, K., Ueno, H., Nakagawa, R., Sato, H., Kondo, E., *et al.* (1997) *Science* **278,** 1626–1629.
10. Wang, B., Geng, Y. B. & Wang, C. R. (2001) *J. Exp. Med.* **194,** 313–320.
11. Sharif, S., Arreaza, G. A., Zucker, P., Mi, Q. S., Sondhi, J., Naidenko, O. V., Kronenberg, M., Koezuka, Y., Delovitch, T. L., Gombert, J. M., *et al.* (2001) *Nat. Med.* **7,** 1057–1062.
12. Hong, S., Wilson, M. T., Serizawa, I., Wu, L., Singh, N., Naidenko, O. V., Miura, T., Haba, T., Scherer, D. C., Wei, J., *et al.* (2001) *Nat. Med.* **7,** 1052–1056.
13. Miyamoto, K., Miyake, S. & Yamamura, T. (2001) *Nature* **413,** 531–534.
14. Mizuno, M., Masumura, M., Tomi, C., Chiba, A., Oki, S., Yamamura, T. & Miyake, S. (2004) *J. Autoimmun.* **23,** 293–300.
15. Sonoda, K. H., Exley, M., Snapper, S., Balk, S. P. & Stein-Streilein, J. (1999) *J. Exp. Med.* **190,** 1215–1226.
16. Cui, J., Shin, T., Kawano, T., Sato, H., Kondo, E., Toura, I., Kaneko, Y., Koseki, H., Kanno, M. & Taniguchi, M. (1997) *Science* **278,** 1623–1626.
17. Behar, S. M., Podrebarac, T. A., Roy, C. J., Wang, C. R. & Brenner, M. B. (1999) *J. Immunol.* **162,** 161–167.
18. Brossay, L., Tangri, S., Bix, M., Cardell, S., Locksley, R. & Kronenberg, M. (1998) *J. Immunol.* **160,** 3681–3688.
19. Prigozy, T. I., Naidenko, O., Qasba, P., Elewaut, D., Brossay, L., Khurana, A., Natori, T., Koezuka, Y., Kulkarni, A. & Kronenberg, M. (2001) *Science* **291,** 664–667.
20. Porcelli, S., Morita, C. T. & Brenner, M. B. (1992) *Nature* **360,** 593–597.
21. Matsuda, J. L., Naidenko, O. V., Gapin, L., Nakayama, T., Taniguchi, M., Wang, C. R., Koezuka, Y. & Kronenberg, M. (2000) *J. Exp. Med.* **192,** 741–754.
22. Pal, E., Tabira, T., Kawano, T., Taniguchi, M., Miyake, S. & Yamamura, T. (2001) *J. Immunol.* **166,** 662–668.
23. Matsuda, J. L., Gapin, L., Baron, J. L., Sidobre, S., Stetson, D. B., Mohrs, M., Locksley, R. M. & Kronenberg, M. (2003) *Proc. Natl. Acad. Sci. USA* **100,** 8395–8400.
24. Crowe, N. Y., Uldrich, A. P., Kyparissoudis, K., Hammond, K. J., Hayakawa, Y., Sidobre, S., Keating, R., Kronenberg, M., Smyth, M. J. & Godfrey, D. I. (2003) *J. Immunol.* **171,** 4020–4027.
25. Wilson, M. T., Johansson, C., Olivares-Villagomez, D., Singh, A. K., Stanic, A. K., Wang, C. R., Joyce, S., Wick, M. J. & Van Kaer, L. (2003) *Proc. Natl. Acad. Sci. USA* **100,** 10913–10918.
26. Carnaud, C., Lee, D., Donnars, O., Park, S. H., Beavis, A., Koezuka, Y. & Bendelac, A. (1999) *J. Immunol.* **163,** 4647–4650.
27. Schmieg, J., Yang, G., Franck, R. W. & Tsuji, M. (2003) *J. Exp. Med.* **198,** 1631–1641.
28. Hayakawa, Y., Takeda, K., Yagita, H., Kakuta, S., Iwakura, Y., Van Kaer, L., Saiki, I. & Okumura, K. (2001) *Eur. J. Immunol.* **31,** 1720–1727.
29. Eberl, G. & MacDonald, H. R. (2000) *Eur. J. Immunol.* **30,** 985–992.
30. Kitamura, H., Ohta, A., Sekimoto, M., Sato, M., Iwakabe, K., Nakui, M., Yahata, T., Meng, H., Koda, T., Nishimura, S., *et al.* (2000) *Cell. Immunol.* **199,** 37–42.
31. Stanic, A. K., Shashidharamurthy, R., Bezbradica, J. S., Matsuki, N., Yoshimura, Y., Miyake, S., Choi, E. Y., Schell, T. D., Van Kaer, L., Tevethia, S. S., *et al.* (2003) *J. Immunol.* **171,** 4539–4551.
32. Benlagha, K., Kyin, T., Beavis, A., Teyton, L. & Bendelac, A. (2002) *Science* **296,** 553–555.
33. Gumperz, J. E., Miyake, S., Yamamura, T. & Brenner, M. B. (2002) *J. Exp. Med.* **195,** 625–636.
34. Lee, P. T., Benlagha, K., Teyton, L. & Bendelac, A. (2002) *J. Exp. Med.* **195,** 637–641.
35. Gadue, P. & Stein, P. L. (2002) *J. Immunol.* **169,** 2397–2406.
36. Pellicci, D. G., Hammond, K. J., Uldrich, A. P., Baxter, A. G., Smyth, M. J. & Godfrey, D. I. (2002) *J. Exp. Med.* **195,** 835–844.
37. Sidobre, S., Naidenko, O. V., Sim, B. C., Gascoigne, N. R., Garcia, K. C. & Kronenberg, M. (2002) *J. Immunol.* **169,** 1340–1348.
38. Kang, S. J. & Cresswell, P. (2004) *Nat. Immunol.* **5,** 175–181.
39. Moody, D. B. & Porcelli, S. A. (2003) *Nat. Rev. Immunol.* **3,** 11–22.
40. Winau, F., Schwierzeck, V., Hurwitz, R., Remmel, N., Sieling, P. A., Modlin, R. L., Porcelli, S. A., Brinkmann, V., Sugita, M., Sandhoff, K., *et al.* (2004) *Nat. Immunol.* **5,** 169–174.
41. Zhou, D., Cantu, C., III, Sagiv, Y., Schrantz, N., Kulkarni, A. B., Qi, X., Mahuran, D. J., Morales, C. R., Grabowski, G. A., Benlagha, K., *et al.* (2004) *Science* **303,** 523–527.
42. Goff, R. D., Gao, Y., Mattner, J., Zhou, D., Yin, N., Cantu, C., III, Teyton, L., Bendelac, A. & Savage, P. B. (2004) *J. Am. Chem. Soc.* **126,** 13602–13603.
43. Oki, S., Chiba, A., Yamamura, T. & Miyake, S. (2004) *J. Clin. Invest.* **113,** 1631–1640.
44. Benish, B., Jullien, D., Dutrone, Y., Huang, B. B., Modlin, R., Spada, F. M., Porcelli, S. A. & Nickoloff, B. J. (2000) *J. Immunol.* **165,** 4076–4085.
45. Colgan, S. P., Pitman, R. S., Nagaishi, T., Mizoguchi, A., Mizoguchi, E., Mayer, L. F., Shao, L., Sartor, R. B., Subjeck, J. R. & Blumberg, R. S. (2003) *J. Clin. Invest.* **112,** 745–754.
46. Brossay, L., Jullien, D., Cardell, S., Sydora, B. C., Burdin, N., Modlin, R. L. & Kronenberg, M. (1997) *J. Immunol.* **159,** 1216–1224.
47. Park, S. H., Roark, J. H. & Bendelac, A. (1998) *J. Immunol.* **160,** 3128–3134.
48. Roark, J. H., Park, S. H., Jayawardena, J., Kavita, U., Shannon, M. & Bendelac, A. (1998) *J. Immunol.* **160,** 3121–3127.
49. Lang, G. A., Malisev, S. D., Besra, G. S. & Lang, M. L. (2004) *Immunology* **112,** 386–396.
50. Buatois, V., Baillet, M., Becart, S., Mooney, N., Leserman, L. & Machy, P. (2003) *J. Immunol.* **171,** 5812–5819.

International Immunology, Vol. 17, No. 12, pp. 1619–1629
doi:10.1093/intimm/dxh342

Preferential T_h2 polarization by OCH is supported by incompetent NKT cell induction of CD40L and following production of inflammatory cytokines by bystander cells *in vivo*

Shinji Oki, Chiharu Tomi, Takashi Yamamura and **Sachiko Miyake**

Department of Immunology, National Institute of Neuroscience, NCNP, 4-1-1 Ogawahigashi, Kodaira, Tokyo 187-8502, Japan

Keywords: cell activation, cytokines, inflammation, natural killer, rodent, T cells

Abstract

The altered glycolipid ligand OCH is a selective inducer of T_h2 cytokines from NKT cells and a potent therapeutic reagent for T_h1-mediated autoimmune diseases. Although we have previously shown the intrinsic molecular mechanism of preferential IL-4 production by OCH-stimulated NKT cells, little is known about the extrinsic regulatory network for IFN-γ production. Here we demonstrate that OCH induces lower production of IFN-γ, not only by NKT cells but also by NK cells compared with α-galactosylceramide. OCH induced lower IL-12 production due to ineffective primary IFN-γ and CD40 ligand expression by NKT cells, and resulted in lower secondary IFN-γ induction. Co-injection of a sub-optimal dose of IFN-γ and stimulatory anti-CD40 mAb compensates for the lower induction of IL-12 by OCH administration. IL-12 converts OCH-induced cytokine expression from IL-4 predominance to IFN-γ predominance. Furthermore, CpG oligodeoxynucleotide augmented IL-12 production when co-administrated with OCH, resulting in increased IFN-γ production. Taken together, the lower IL-12 production and subsequent lack of secondary IFN-γ burst support the effective T_h2 polarization of T cells by OCH. In addition, highlighted in this study is the characteristic property of OCH that can induce the differential production of IFN-γ or IL-4 according to the availability of IL-12.

Introduction

NKT cells are a unique subset of CD1d-restricted T lymphocytes that express TCR and some NKR. NKT cells recognize glycolipid antigens such as α-galactosylceramide (αGC) by an invariant TCRα chain composed of Vα14-Jα18 segments in mice and Vα24-Jα18 segments in humans, associated with TCRβ chains using a restricted set of Vβ genes (1, 2). NKT cells rapidly secrete large amounts of cytokines including IL-4 and IFN-γ upon antigen stimulation and are effective regulators of T_h1/T_h2 balance *in vivo* (3–5). We have previously demonstrated that *in vivo* administration to mice of altered glycolipid ligand, OCH, ameliorates experimental autoimmune encephalomyelitis (EAE), collagen-induced arthritis (CIA) and type I diabetes by enhancing IL-4-dependent T_h2 responses without inducing IFN-γ production and pathogenic T_h1 responses (6–8).

Recently, we have clarified the intrinsic molecular mechanism of preferential IL-4 production by OCH-stimulated NKT cells (9). IFN-γ production by NKT cells was more susceptible to the sphingosine length of glycolipid ligand than that of IL-4, and the length of sphingosine chain determined the half-life of NKT cell stimulation by CD1d-associated glycolipids. IFN-γ production by NKT cells required longer T cell stimulation than did IL-4 production and the transcription of the IFN-γ gene required *de novo* protein synthesis by activated NKT cells. The NF-κB family member transcription factor c-Rel was preferentially transcribed in αGC-stimulated, but not in OCH-stimulated, NKT cells and was identified as essential for IFN-γ production by activated NKT cells. Therefore, the differential duration of NKT cell stimulation, due to the binding stability of individual glycolipid antigens to CD1d molecules, determines whether signaling leads to effective c-Rel transcription and IFN-γ production by activated NKT cells.

Upon stimulation by αGC *in vivo*, NKT cells rapidly affect the functions of neighboring cell populations such as T cells, NK cells, B cells and dendritic cells (DCs) in a direct or indirect manner (10–13). The serial production of IFN-γ by NKT cells

Correspondence to: S. Miyake; E-mail: miyake@ncnp.go.jp

Transmitting editor: K. Okumura

Received 19 August 2005, *accepted* 30 September 2005

Advance Access publication 15 November 2005

and NK cells has been demonstrated, suggesting that activated NKT cells may influence further IFN-γ production by other cells including NK cells (3, 10). A C-glycoside analog of αGC has been shown to induce a superior T_h1-type response than αGC does by inducing higher IFN-γ production by NK cells. IL-12 was indispensable for the T_h1-skewing effect of the glycolipid, indicating the importance of IL-12 in enhanced IFN-γ production *in vivo* (14). Furthermore, αGC-stimulated NKT cells can act as an adjuvant *in vivo* by inducing the full maturation of DCs, as manifested by augmented co-stimulatory molecules and enhanced mixed leukocyte reactions (11). Accordingly, αGC-stimulated NKT cells were shown to express CD40 ligand (CD40L, CD154), which can engage CD40 on antigen-presenting cells and stimulate them to produce IL-12 (15, 16). Furthermore, IFN-γ production and T_h1-type responses were impaired in CD40-deficient mice (5). A growing body of evidence suggests that both extrinsic and intrinsic factors compose an intricate network for controlling IFN-γ production and T_h1 polarization after intensive stimulation of NKT cells by superagonistic glycolipid such as αGC.

Although the intrinsic molecular mechanism of preferential IL-4 production by OCH-stimulated NKT cells has been elucidated, little is known about the effect of OCH on bystander cells and the extrinsic regulatory network for IFN-γ production and T_h1 polarization. Considering the lower IFN-γ production by OCH compared with extensive IFN-γ production by αGC *in vivo*, OCH may affect the functions of neighboring cell populations in a different manner from that of αGC. In the current study, we demonstrate that OCH induces less effective production of IFN-γ and IL-12 by bystander cells possibly due to lower expression of CD40L by NKT cells. Co-administration of stimulatory anti-CD40 mAb in combination with IFN-γ enhanced the production of IL-12 induced by OCH *in vivo*, and IL-12 modulated OCH-induced cytokine expression by augmenting IFN-γ. Consistent with these results, co-administration of CpG oligodeoxynucleotide (ODN) with OCH preferentially induced IFN-γ production possibly through augmented IL-12 production. Considering that NKT cell responses to CD1d-presented self-antigens are modified by IL-12 to induce massive IFN-γ production during the course of microbial infection (17), OCH, at least partly, mimics the physiological behavior of the putative self-antigen for NKT cells in the context of cytokine milieu *in vivo*.

Methods

Reagents and antibodies

Murine IL-12, IFN-γ and Flt3-ligand (Flt3L) were purchased from Peprotech EC (London, UK). Anti-CD40 mAb (HM40-3) was purchased from BD Biosciences PharMingen (San Diego, CA, USA). Mouse anti-IFN-γ (R4-6A2) was purified from ascites of hybridoma obtained from American Type Culture Collection. Glycolipids were solubilized in dimethyl sulfoxide (100 μg ml^{-1}) and stored at −20°C until use. The following CpG ODN was synthesized: CpG ODN, 5′-GCATGACGTT-GAGCT-3′.

Mice

C57BL/6 (B6) mice were purchased from CLEA Laboratory Animal Corporation (Tokyo, Japan). MHC class II-deficient I-A^bβ−/− mice with the B6 background were purchased from Taconic (Germantown, NY, USA). All animals were kept under specific pathogen-free conditions and used at 7–12 weeks of age. Animal care and use were in accordance with institutional guidelines.

Induction of bone marrow-derived DCs

Bone marrow cells were isolated by flushing femurs of B6 mice and re-suspended in culture medium supplemented with murine Flt3L (100 ng ml^{-1}) as described in (18). Cells were harvested from the culture after 10 days and subjected to co-culture experiment with NKT cells.

Flow cytometry and intracellular cytokine staining

Spleen cells or liver mononuclear cells harvested after stimulation with glycolipids *in vivo* were cultured in complete media containing GolgiStop (BD PharMingen, San Jose, CA, USA). Then cells were incubated with Fc block (anti-mouse FcγIIR/IIR mAb clone 2.4G2) and were stained with biotinylated anti-NK1.1 mAb (PK136), washed with PBS and then stained with peridinin chlorophyll protein/cyanine 5.5–anti-CD3 mAb and streptavidin–allophycoerythrin (APC). Then cells were washed twice with PBS and fixed in BD Cytofix/Cytoperm solution for 20 min at 4°C. After fixation, cells were washed with BD Perm/Wash solution and re-suspended in the same solution containing either PE–anti-IFN-γ mAb (XMG1.2) or PE-conjugated isotype control Ig for 30 min at 4°C. Then samples were washed and the stained cells were analyzed using a FACS Calibur instrument (Becton Dickinson) with CELLQuest software (Becton Dickinson). Identification of iNKT cells by Dimer X! Recombinant Soluble Dimeric Mouse CD1d (BD PharMingen) was performed as described previously (19). For analysis of CD40L expression, spleen cells harvested after stimulation with glycolipids *in vivo* for indicated periods of time were cultured in complete media containing biotinylated anti-CD40L mAb (MR1) for 2 h. Cells were harvested, washed with PBS and stained with FITC–anti-CD3 mAb, PE–anti-NK1.1 mAb and streptavidin–APC for 20 min. CD40L expression was analyzed in CD3/NK1.1 double-positive cell.

Microarray

Microarray analysis was performed as described previously (9). In brief, I-A^bβ−/− mice pre-treated with anti-asialo GM_1 antibody were injected with αGC or OCH (100 μg kg^{-1}). Total RNA was isolated from liver NKT cells (purified as CD3+ NK1.1+ cells) and applied to microarray by using U74Av2 arrays (GeneChip System, Affymetrix, Santa Clara, CA, USA). From data image files, gene transcript levels were determined using algorithms in the GeneChip Analysis Suit software (Affymetrix).

Quantitative reverse transcription–PCR

Quantitative reverse transcription–PCR was conducted using a Light Cycler-FastStart DNA Master SYBR Green I kit (Roche Molecular Biochemicals) as described previously (9). Primers used for the analysis of gene expression are as follows; CD40L (F) CGAGTCAACGCCCATTCATC, (R) GTAATTCAAA-CACTCCGCCC.

ELISA

The level of cytokine production in cell culture supernatants or in serum was evaluated by standard sandwich ELISA, employing purified and biotinylated mAb sets (11B11/BVD6-24G2 for IL-4, R4-6A2/XMG1.2 for IFN-γ and 9A5/C17.8 for IL-12) and standards (OptEIA set, BD PharMingen) as described previously (9). After adding a substrate, the reaction was evaluated using a Microplate reader (BioRad).

Statistics

For statistic analysis, non-parametric Mann–Whitney test was used to calculate significance levels for all measurements. Values of $P < 0.05$ was considered statistically significant.

Results

OCH induces lower IFN-γ expression than αGC in both NKT cells and NK cells in vivo

Although NKT cells are a major source of IL-4 after glycolipid administration *in vivo*, activated NKT cells are shown to affect the functions of bystander cells such as T cells, NK cells, B cells and DCs in a direct or indirect manner, resulting in possible secondary augmentation of IFN-γ production by these cells. To evaluate the contribution of NKT cells and other cells for IFN-γ production after glycolipid administration, we performed kinetic analysis of cytokine production by splenic NKT cells, NK cells, T cells and other cells after *in vivo* administration of glycolipids. IFN-γ production was detected both in NKT cells and NK cells (Fig. 1A), and neither CD3+ T cells nor CD3−NK1.1− cells showed significant IFN-γ production 2 or 6 h after glycolipid administration. αGC induced a larger population of IFN-γ-producing NKT cells than OCH did which is consistent with the previous report (9). The kinetic analysis revealed that IFN-γ production by NKT cells was dominant in earlier time points (2 h) after glycolipid administration and IFN-γ production by NK cells was comparable or even higher at later time points (6 h) (Fig. 1B), suggesting that IFN-γ production by NKT cells preceded IFN-γ production by NK cells as reported previously (3, 10). As CD3+NK1.1+ cells do not always represent CD1d-restricted iNKT cells, we compared IFN-γ production by CD1d-dimerX-positive T cells after treatment with αGC or OCH. Again, αGC induced a larger population of IFN-γ-producing iNKT cells than OCH did (Fig. 1C). Interestingly, αGC induced a much larger population of IFN-γ-producing NK cells than

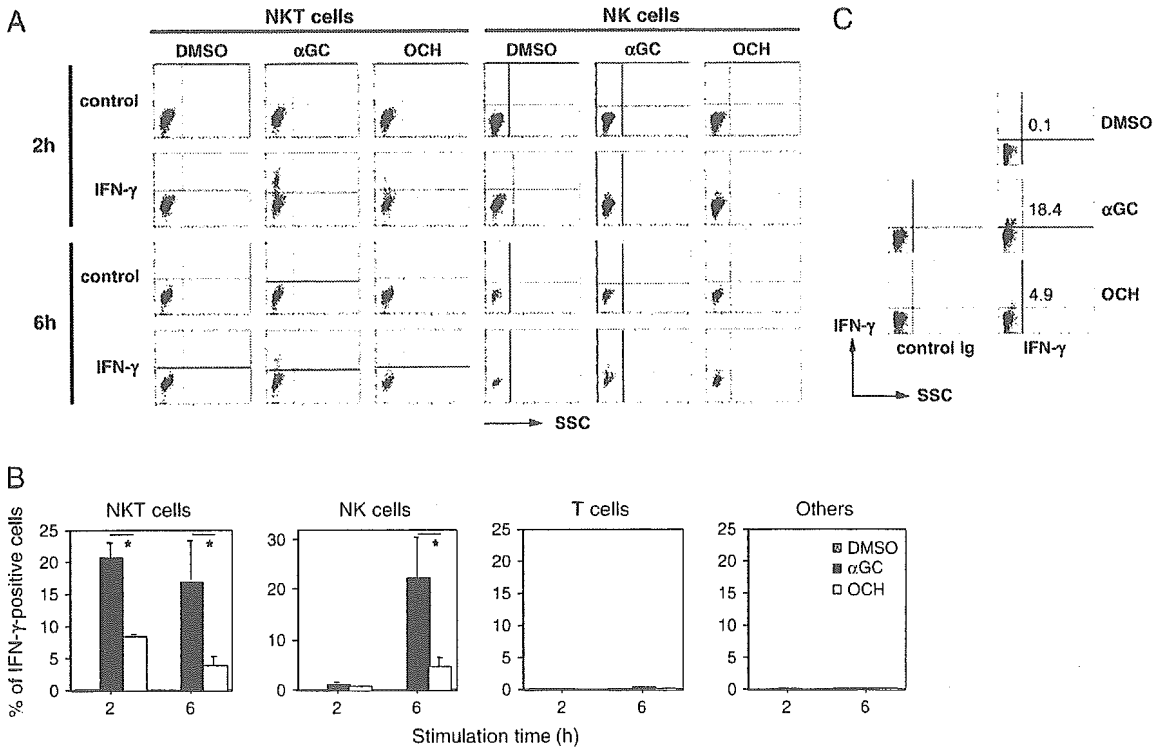

Fig. 1. Expression of IFN-γ by NKT cells and non-NKT cells after administration of glycolipid ligands. B6 mice were treated intra-peritoneally with 2 μg per mouse of either αGC or OCH, and spleen cells were harvested at various time points after glycolipid administration and subjected to intracellular cytokine staining as described in Methods. (A) Data analyzed for CD3+NK1.1+ NKT cells, CD3−NK1.1+ NK cells, CD3+NK1.1− T cells and CD3−NK1.1− cells were shown for the presence of intracellular IFN-γ. Similar results were obtained by analyzing liver mononuclear cells after glycolipid administration (data not shown). (B) Plotted values represent the percentage of IFN-γ-positive cells (mean ± SD for triplicate samples) in the gated population after treatment with dimethyl sulfoxide (DMSO) (hatched bar), αGC (filled bar), or OCH (open bar). (C) Data analyzed for CD1d-DimerX-positive iNKT cells were shown for the presence of intracellular IFN-γ 2 h after glycolipid treatment. The experiments shown are representative of three independent experiments. $^*P < 0.05$.

OCH, suggesting that OCH induces less IFN-γ production than αGC not only by direct effect on NKT cells but also by indirect effect on NK cells. To exclude the possibility of the contamination of activated non-CD1d-restricted T cells into NKT fractions or activated NKT cells into NK cells fraction due to the down-regulation of TCR, we conducted the following experiments. First, αGC-loaded DimerXI-stained cells were concentrated in the NK1.1+CD3+ population and <0.4% of cells were reactive to αGC-loaded DimerXI either in NK1.1+CD3− or NK1.1−CD3+ cell populations. Second, >95% of αGC-loaded DimerXI-reactive spleen cells were positive for both CD3 and NK1.1 after stimulation with glycolipids. Third, most of the intracellular IFN-γ-positive CD3− cells were DX5 positive 2 and 6 h after stimulation with glycolipids (data not shown). These results indicated that the contamination of IFN-γ-producing cells into the other fractions was minimum.

αGC-induced IFN-γ production by NK cells is partly dependent on IFN-γ produced by NKT cells

To determine the effect of IFN-γ on consequent IFN-γ production by NK cells, we treated mice with anti-IFN-γ mAb before administration of αGC, and then examined IFN-γ-producing cells using intracellular staining. As shown in Fig. 2, there was no significant difference in the frequency of IFN-γ-producing NKT cells after administration of αGC with or without anti-IFN-γ mAb. Meanwhile, co-administration of anti-IFN-γ mAb showed ~35% reduction in IFN-γ-producing NK cells after αGC treatment (Fig. 2, right panel). These results suggested that NKT cell-derived IFN-γ was involved in αGC-induced IFN-γ production by NK cells to some extent, but an IFN-γ-independent mechanism might be involved in indirect up-regulation of IFN-γ production by NK cells after αGC administration *in vivo*.

OCH administration does not induce effective IL-12 production

As DCs were demonstrated to be activated after *in vivo* administration of αGC (11, 20) to produce large amount of IL-12 (21) and IL-12 is one of the most potent inducers of IFN-γ (22), we performed kinetic cytokine analysis of serum levels of IL-12 (p70) together with IFN-γ and IL-4 after intraperitoneal injection of the glycolipids into B6 mice. As shown in Fig. 3, administration of αGC induced a rapid elevation of IL-4 and a delayed elevation of IFN-γ in B6 mice. In contrast, administration of OCH induced a rapid elevation of IL-4 comparable to that induced by αGC with significantly less amount of elevation of IFN-γ, resulted in T_h2 skewing as described previously. Although the level of IL-12 in serum was observed 6 h after αGC injection, OCH injection induced one-tenth amount of serum IL-12 level compared with αGC. In addition, freshly isolated liver NKT cells co-cultured with Flt3L-induced DCs produced significantly higher amount of IL-12 in the presence of αGC compared with OCH. Meanwhile, Flt3L-induced DCs loaded with either αGC or OCH exerted comparable amount of IL-4 production (Fig. 3B), demonstrating directly that DCs loaded with OCH produce less IL-12 upon co-culture with NKT cells than DCs loaded with αGC, and therefore suggest that the *in vivo* effects of OCH are not simply due to its preferential presentation by antigen-presenting cells that produce less IL-12. Taken together, these results indicated that OCH administration did not induce effective IL-12 production *in vivo*.

Lower expression of CD40L on OCH-stimulated NKT cells

Activated NKT cells stimulate DCs to produce IL-12 through the engagement of CD40 on DCs with CD40L inducibly expressed on NKT cells (15, 21). Furthermore, a C-glycoside analog of αGC induced a superior IFN-γ production by NK cells than αGC does in an IL-12-dependent manner (14),

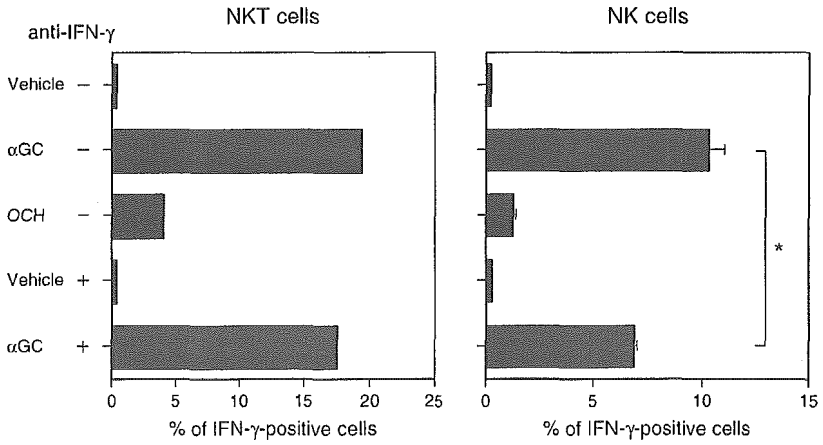

Fig. 2. αGC-induced IFN-γ production by NK cells is partly dependent on IFN-γ production by NKT cells. B6 mice were treated intra-peritoneally with 2 μg per mouse of glycolipids with or without 500 μg per mouse of anti-IFN-γ mAb. Four hours after treatment, spleen cells were harvested and subjected to intracellular cytokine staining. Plotted values represent the percentage of IFN-γ-positive cells (mean ± SD for triplicate samples) in the gated population for CD3+NK1.1+ NKT cells (left) or CD3−NK1.1+ NK cells (right). Similar results were obtained by analyzing liver mononuclear cells after glycolipid administration (data not shown). The experiments shown are representative of three independent experiments. *$P < 0.05$.

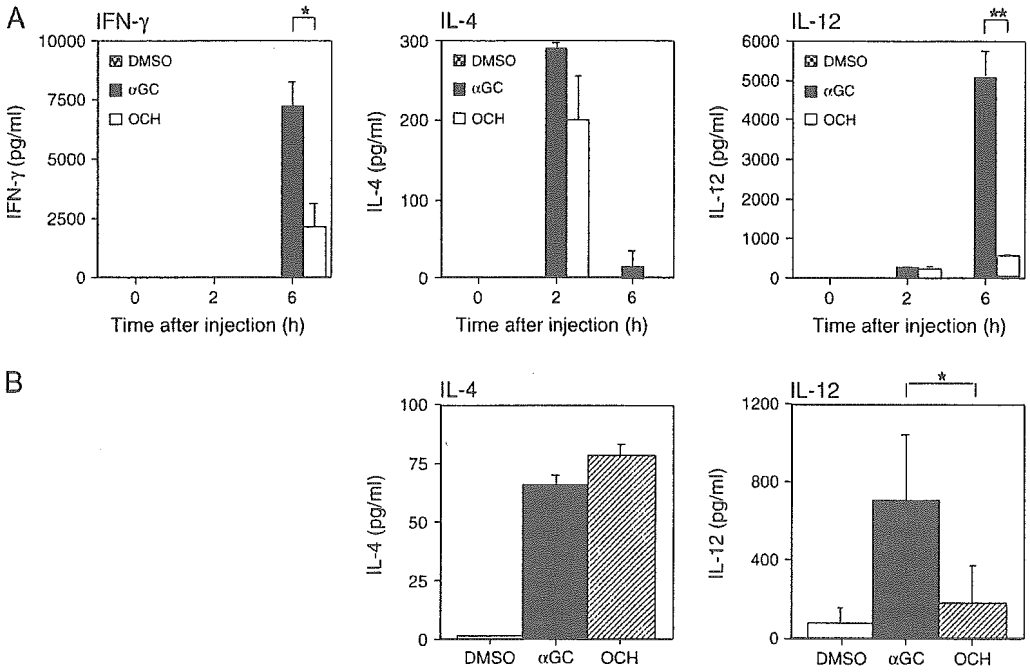

Fig. 3. OCH administration does not induce effective IL-12 production. (A) B6 mice were injected intra-peritoneally with vehicle alone, 2 μg per mouse of αGC or OCH and serum samples were collected at indicated times after injection. Serum levels of IFN-γ, IL-4 and IL-12 (mean ± SD) were determined by ELISA. This figure represents one of two experiments with similar results. $*P < 0.05$, $**P < 0.01$. (B) Freshly isolated liver NKT cells were co-cultured with Flt3L-induced DCs in the presence of αGC or OCH for 72 h. Levels of IL-4 and IL-12 were determined by ELISA. Data are expressed as mean ± SD for triplicate wells and representative data of two similar experiments are shown. $*P < 0.05$.

which suggests that IFN-γ production by NK cells might be regulated by IL-12. To clarify the mechanisms of lack of IL-12 production upon stimulation with OCH, we compared the inducible expression of CD40L on NKT cells after *in vivo* administration of glycolipids. Microarray analysis revealed that CD40L transcripts were inducibly expressed in NKT cells 1.5 h after stimulation with αGC and disappeared 12 h after stimulation. In contrast, OCH treatment induced approximately one-third of CD40L transcription compared with the effect of αGC (Fig. 4A). Consistent with the data of microarray analysis, real-time PCR analysis confirmed the preferential up-regulation of CD40L transcript after αGC stimulation (Fig. 4B). To demonstrate the differential expression of CD40L between αGC-stimulated and OCH-stimulated NKT cells, surface expression of CD40L on NKT cells were compared by flow cytometry after *in vivo* treatment with the glycolipids. As shown in Fig. 4(C), αGC induced higher expression of CD40L than OCH did on the surface of NKT cells. If compared quantitatively by mean fluorescence intensity of CD40L-positive subsets after treatment with either glycolipid, OCH treatment induced less CD40L expression on NKT cells compared with the effect of αGC (Fig. 4C, right panel). These results indicated that CD40L expression on αGC-stimulated NKT cells was significantly higher than that on OCH-stimulated NKT cells.

Co-administration of IFN-γ and CD40 stimulation augments IL-12 production by OCH in vivo

Although the CD40 pathway plays an intrinsic role in physiological conditions in eliciting IL-12 production, effective production of bioactive IL-12 by DCs requires another signal mediated by innate signals such as microbial stimuli (23) or by IFN-γ (24–26). Therefore, OCH-induced expression of CD40L and IFN-γ may not be effective to initiate IL-12 production from DCs *in vivo*. To test this hypothesis, we examined whether co-administration of stimulatory anti-CD40 mAb and/or IFN-γ confer OCH to induce higher IL-12 production. As shown in Fig. 5, administration of IFN-γ, stimulatory anti-CD40 mAb or combination of both reagents did not induce IL-12 expression *in vivo*. On the contrary, OCH-induced IL-12 production was partially augmented by co-administration of anti-CD40 mAb. Furthermore, concomitant administration of IFN-γ and stimulatory anti-CD40 mAb with OCH induced IL-12 production. These results suggest that the signals through CD40 and IFN-γ provided by OCH-stimulated NKT cells did not lead to efficient production of IL-12.

Co-administration of IL-12 augments IFN-γ production by OCH in vivo

A series of experiments so far indicated that OCH was less effective for induction of CD40L, IFN-γ and consequent IL-12 production than those induced by αGC. To examine directly the role of IL-12 production in less effective IFN-γ production by NKT cells and NK cells after OCH administration, we tested whether co-administration of IL-12 with OCH induces IFN-γ *in vitro* and *in vivo*. As shown in Fig. 6(A), IL-12 augmented IFN-γ production from spleen cells after *in vitro* treatment with

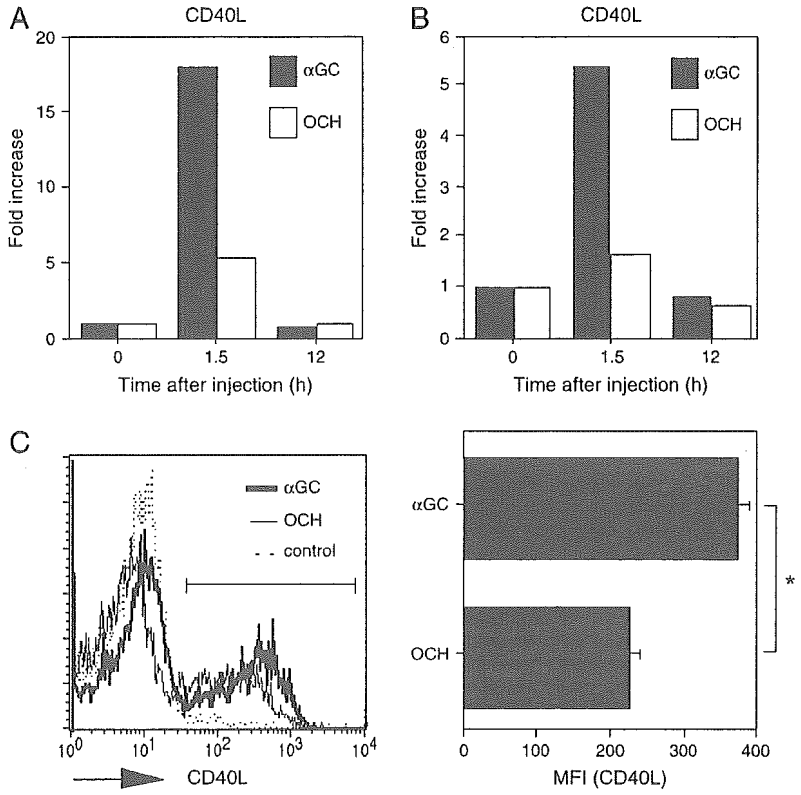

Fig. 4. Expression of CD40L on NKT cells stimulated with αGC or OCH. (A) Plotted values represent data of Affymetrix microarray analysis for indicated genes. The αGC- or OCH-stimulated liver NKT cells (purified as CD3+ NK1.1+ cells) as well as unstimulated NKT cells were analyzed at the indicated time points and the data represent to the relative values for glycolipid-treated samples when the value in NKT cells derived from untreated animals was defined as 1. (B) Real-time PCR analysis for the expression of CD40L mRNA. Data are presented as a fold induction of cytokine mRNAs after glycolipid treatment. The amount of mRNA in NKT cells derived from untreated animals was defined as 1. (C) Cell-surface expression of CD40L on αGC-stimulated (bold line) or OCH-stimulated (thin line) NKT cells. CD40L expression was analyzed in CD3/NK1.1 double-positive cell. Dotted line represents the histogram of control staining. B6 mice were injected intra-peritoneally with either αGC or OCH and liver mononuclear cells were isolated at the indicated time point. Cell-surface expression of CD40L was analyzed by flow cytometry (left) and plotted (right) as mean fluorescence intensity (MFI). Data are expressed as mean ± SD for duplicate samples. This figure represents one of two experiments with similar results. $*P < 0.05$.

OCH in a dose-dependent manner. Higher doses of IL-12 induced IFN-γ production even without OCH and the effect of OCH is concealed in this condition. Interestingly, IL-12 treatment inhibits IL-4 production by OCH-stimulated spleen cells in a dose-dependent manner, suggesting the reciprocal regulation of cytokine production by IL-12. Next we examined the effect of co-administration of sub-optimal dose of IL-12 together with OCH. As shown in Fig. 6(B), co-administration of OCH and IL-12 induced significantly higher production of IFN-γ compared with either treatment alone, although sub-optimal dose of IL-12 alone failed to induce IFN-γ production. In contrast, co-administration of IL-12 did not enhance the IL-4 production 2 h after OCH administration *in vivo*. As both NKT cells and NK cells are important sources of IFN-γ after glycolipid stimulation, we evaluated the frequency of IFN-γ-producing NKT and NK cells after co-administration of OCH with IL-12. As shown in Fig. 6(C), IL-12 augmented the proportions of IFN-γ-producing cells in both cell populations, but not in conventional T cells, when co-administered with OCH. These results demonstrated that the properties of OCH for less effective IFN-γ production by NKT cells and NK cells could be compensated by co-administration of IL-12.

Modification of cytokine profiles by pathogen-associated molecular patterns after OCH treatment in vivo

As sub-optimal dose of IL-12 was able to rescue defective IFN-γ production by administration of OCH alone, availability of IL-12 might be a crucial determinant for OCH-induced production of IFN-γ. As DCs and phagocytes produce IL-12 in response to pathogens during infection, pathogen-associated molecular patterns (PAMPs) are possible important determinants for cytokine profiles after OCH stimulation *in vivo*. We applied CpG ODN (27), which skews the host's immune milieu in favor of T_h1 responses by enhancing the production of pro-inflammatory cytokines including IL-12 (28), for analyzing cytokine profile of OCH. As shown in Fig. 7(A), CpG ODN alone induced no cytokine production within 6 h after injection. Concomitant injection of CpG ODN with OCH induced strong IFN-γ production (7.5-fold induction with 10 μg per mouse of CpG ODN plus OCH and 14-fold induction with 100 μg per

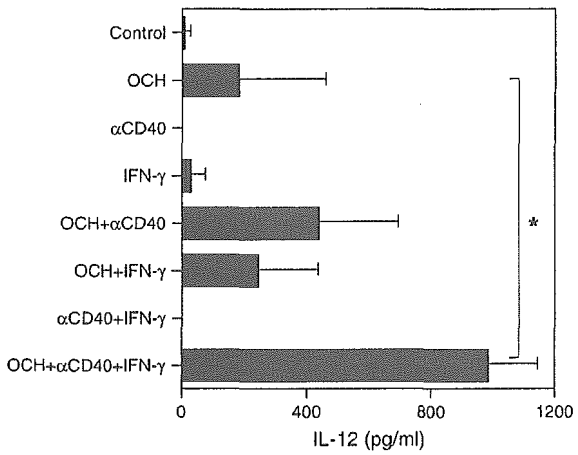

Fig. 5. Co-administration of IFN-γ and stimulatory anti-CD40 mAb augments IL-12 production after OCH administration *in vivo*. B6 mice were treated intra-peritoneally with 2 μg per mouse of glycolipids in combination with murine IFN-γ (1 μg per mouse) and/or stimulatory anti-CD40 mAb (100 μg per mouse) and serum samples were collected 2 h after treatment. The level of IL-12 production was determined by ELISA. These data represent one of two experiments with similar results. $^*P < 0.05$.

mouse of CpG ODN plus OCH) and induced moderate IL-4 production (2.6-fold induction with 10 μg per mouse of CpG ODN plus OCH and 2.1-fold induction with 100 μg per mouse of CpG ODN plus OCH). Accordingly, co-administration of OCH and 10 μg per mouse of CpG ODN exhibited strong induction of IL-12 production (Fig. 7B, left panel), suggesting the synergic effect of OCH and CpG ODN for preferential up-regulation of IL-12. These results suggested that the PAMPs could be a considerable determinant for the cytokine profile following *in vivo* administration of OCH through regulating the availability of pro-inflammatory cytokines such as IL-12.

Discussion

In this study, we clarified the effect of OCH on bystander cell activation including the sequential IFN-γ production by NK cells and the functional conditioning of DCs. *In vivo* administration of OCH induced much lower IFN-γ production from both NKT and NK cells compared with that induced by αGC administration. NKT cell-derived IFN-γ was partially involved in inducing IFN-γ production by NK cells after αGC administration, implying that an IFN-γ-independent mechanism is also important for indirect up-regulation of IFN-γ production by NK cells after αGC administration *in vivo*. OCH administration induced lower CD40L expression by NKT cells compared with αGC administration, resulting in the lower production of IL-12 by DCs. Co-injection of stimulatory CD40 mAb and IFN-γ with OCH augmented the OCH-induced IL-12 production. Likewise, co-injection of IL-12 with OCH enhanced the production of IFN-γ by OCH administration alone. Furthermore, administration of OCH and CpG ODN into mice selectively induced IFN-γ production *in vivo*.

Consistent with the previous reports (9, 29), we here demonstrated that OCH administration induced less amount of IFN-γ than that of αGC in iNKT cells. Supporting these observation is another report in which truncation of the phytosphingosine lipid chain of αGC increases the relative amounts of IL-4 release by human NKT cells (30).

The functional relevance between NKT cells and NK cells was demonstrated in which NK-sensitive tumor incidence was higher and the time of tumor development was earlier in NKT cell-deficient mice compared with B6 mice (31). Considering that NKT cell-deficient mice still possess NK cells (32), NKT cells might serve as a modulator of NK cell function in tumor immunity, though the molecular mechanisms of how NKT cells modulate NK cells has not been clarified yet. Recently, β-anomeric galactosylceramide has been reported to have a capacity to reduce numbers of NKT cells without inducing typical NK cell-mediated responses (29, 33). We demonstrated in this study that OCH-induced IFN-γ production by NK cells was lower compared with that induced by αGC. This is at least partly due to the lower induction of IFN-γ by OCH-stimulated NKT cells and the lower induction of IL-12 by DCs, leading to weak activation of NK cells. There is a report showing that OCH and αGC can induce comparable amount of IFN-γ by NK cells 8 and 24 h after stimulation (29), even though serum levels of IFN-γ induced by OCH treatment were significantly lower than that by αGC treatment 6 or 24 h after stimulation. Since the major producer of IFN-γ *in vivo* after treatment with glycolipids at the later time points were demonstrated to be NK cells (3, 10), it is not clear whether cells other than NKT cells or NK cells could be the IFN-γ producer after αGC stimulation in their experimental condition. Although the basis for the discrepancy is not clear, it may be related to the difference in the synthetic methods of those glycolipids. Nevertheless, we reproducibly confirmed the *in vivo* ameliorating effects of OCH in various autoimmune mouse models including EAE, CIA and inflammatory bowel disease (7, 8, 34) through the differential induction of various cytokines.

The CD40 pathway plays an intrinsic role in physiological conditions by eliciting IL-12 production by DCs (35, 36). However, cross-linking of CD40 alone has been shown to be incapable of inducing IL-12 production by DCs. Schulz *et al.* (23) has demonstrated that effective production of bioactive IL-12 by DCs through T cell activation should be initiated by innate signals such as microbial stimuli. Activated T cell-mediated IL-12 production by DCs through CD40 signaling requires another signal, for example, IFN-γ (24–26), which is also shown to be required for uncommitted immature DCs to develop the capacity to produce high levels of IL-12 upon subsequent contact with naive T cells (25). Consistent with the observation, IFN-γ enhances gene transcription encoding both the p40 and p35 components of IL-12, resulting in a particularly marked production of the heterodimeric IL-12 (37, 38). Intriguingly, αGC-induced expression of IL-12R on NKT cells requires the production of IFN-γ by NKT cells and the production of IL-12 by DCs (21). In addition, IL-12 itself has been shown to act directly on DCs to promote IL-12 production (39). αGC provides dual signals to DCs by up-regulating CD40L on NKT cells and by inducing IFN-γ production by NKT cells, resulting in a large amount of IL-12 production by DCs. Our reconstitution experiment clearly showed that signals through CD40 and IFN-γ provided by OCH lead to small

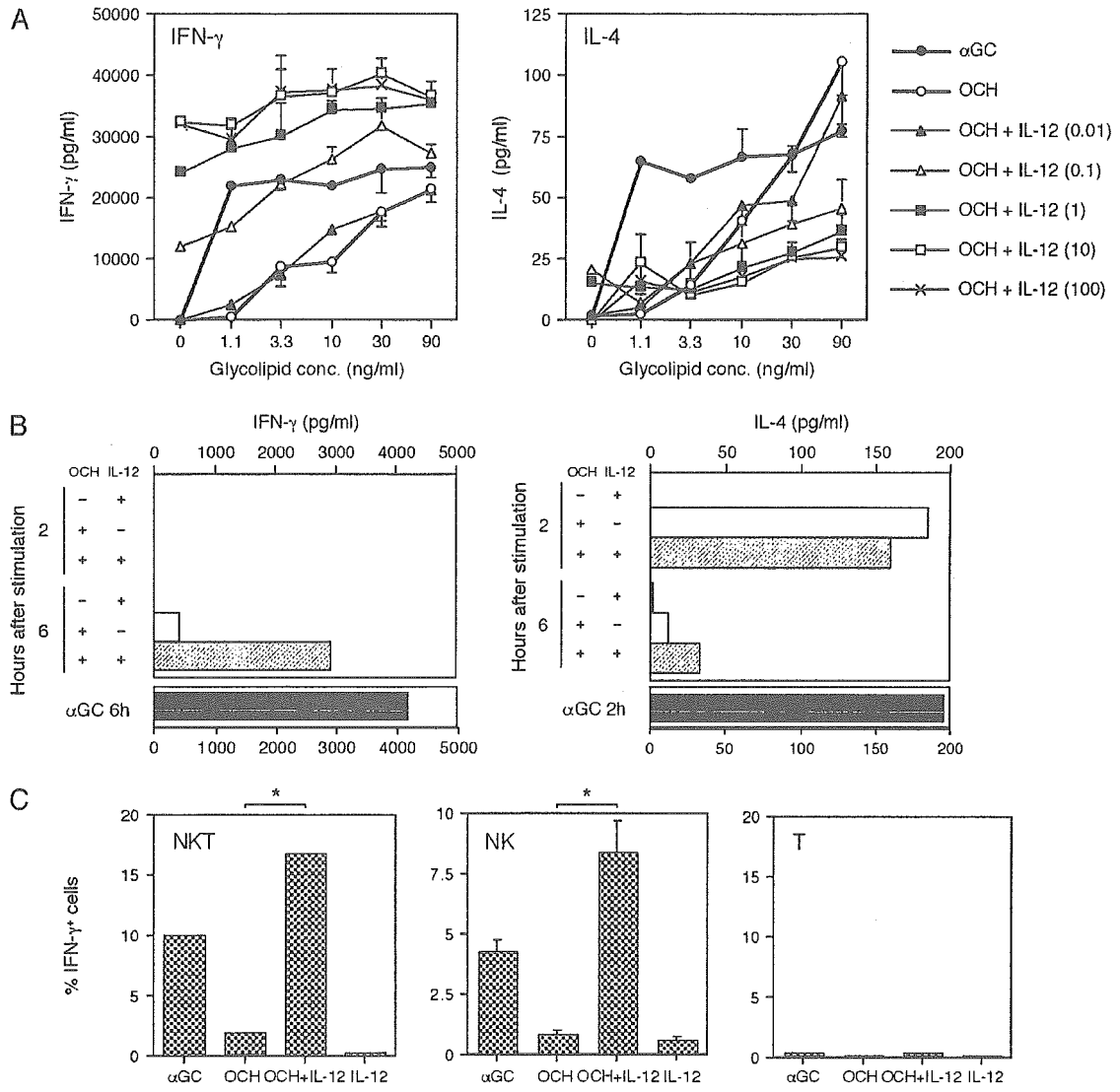

Fig. 6. Co-administration of IL-12 augments IFN-γ production by OCH. (A) Effects of IL-12 on cytokine production of splenocytes stimulated with glycolipids *in vitro*. Splenocytes were stimulated with various concentration of αGC or OCH in the presence or absence of IL-12 (with concentrations from 0.01 to 100 ng ml^{-1}) for 72 h and the levels of IFN-γ (left) or IL-4 (right) in the supernatants were measured by ELISA. Data are expressed as mean ± SD for triplicate wells. This figure represents one of two experiments with similar results. (B) Effects of IL-12 on cytokine production after glycolipid administration *in vivo*. B6 mice were treated with 10 ng per mouse of IL-12, 2 μg per mouse of OCH or OCH plus IL-12 and serum samples were collected at indicated times after injection. Serum levels of IFN-γ (left) and IL-4 (right) were determined by ELISA. This figure represents one of three experiments with similar results. (C) B6 mice were treated with 100 ng per mouse of IL-12 alone or in combination with 2 μg per mouse of OCH and spleen cells were harvested at various time points after glycolipid administration and subjected to intracellular cytokine staining as described in Methods. NKT cells, NK cells and T cells were analyzed for the presence of intracellular IFN-γ as described in Fig. 1. Similar results were obtained by analyzing liver mononuclear cells after glycolipid administration (data not shown). Data are expressed as mean ± SD for triplicate wells and represent one of two experiments with similar results. $^*P < 0.05$.

amount of IL-12 production from DCs that is unable to trigger the IFN-γ burst by NKT cells and NK cells.

Treatment of mice with OCH together with sub-optimal doses of IL-12 resulted in significantly augmented IFN-γ production *in vivo*, indicating that the impaired IL-12 production by OCH is likely to be one of the major causes for less effective IFN-γ production *in vivo*. Similar observations were reported previously, in which treatment of mice with sub-optimal doses of αGC together with sub-optimal doses of IL-12 resulted in strongly enhanced natural killing activity and IFN-γ production (21). These results indicate an important role for DC-derived IL-12 for glycolipid-induced activation of NKT cells and suggest that NKT cells may be able to condition DCs for subsequent immune responses. To further clarify the

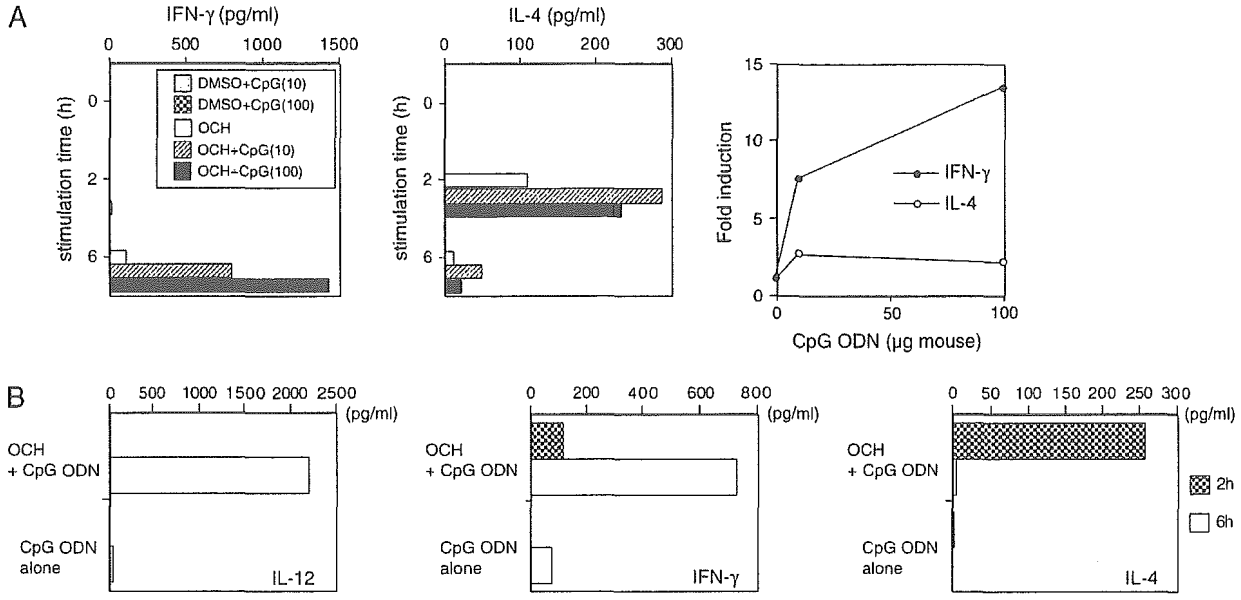

Fig. 7. Co-administration of CpG ODN augments IFN-γ production by OCH stimulation *in vivo*. (A) B6 mice were injected with 10 μg per mouse or 100 μg per mouse of CpG ODN alone or in combination with 2 μg per mouse of OCH and serum samples were collected at indicated times after injection. Serum levels of IFN-γ (left) or IL-4 (center) were determined by ELISA. The ratio of cytokine production was plotted in the right panel as fold induction for IFN-γ (at 6 h after injection) and IL-4 (at 2 h after injection). This figure represents one of two experiments with similar results. (B) B6 mice were injected with 10 μg per mouse of CpG ODN alone or in combination with 2 μg per mouse of OCH and serum samples were collected at indicated times after injection. Serum levels of IL-12 (left), IFN-γ (center) or IL-4 (right) were determined by ELISA. This figure represents one of three experiments with similar results.

cooperative roles of IL-12 for effective IFN-γ production by glycolipid-stimulated NKT cells, CpG ODN (27) was co-administered with OCH, in which IFN-γ production was preferentially augmented in response to IL-12 expression. CpG ODN induces innate immune responses similar to bacterial DNA, and is one of the PAMPs expressed by a diverse group of microorganisms. Taken together, a variety of glycolipid antigens elicit differential effects, not only on NKT cells but also on bystander cells such as NK cells and DCs, which may modulate subsequent immune responses. Recently, Brigl *et al.* demonstrated that a bacterial infection can induce a predominantly T_h1 cytokine responses from self-antigen-primed NKT cells. In this instance, microbial products were recognized not by NKT cells directly, but by DCs, resulting in IL-12 secretion and subsequent potent IFN-γ production (17). Following the exposure of immune cells to exogenous antigens or infection, IL-12 is produced by DCs in response to CD40 signals or microbial products, and co-stimulates the responses of NKT cells to self-antigens, resulting in a significant augmentation of IFN-γ production but no detectable IL-4 production (40). It is noteworthy to point out that the behavior of OCH in response to IL-12 is analogous to that of the putative self-antigen for NKT cells (Fig. 6). Therefore, NKT cells also respond to OCH in a diverse manner according to the availability of IL-12, which can be induced by a wide variety of pathogens, and thus OCH may be a useful tool to evaluate the physiological responses of NKT cells to various innate immune conditions.

Regarding the predominant effect of OCH on T_h2 polarization by NKT cells, several molecules have been identified that positively regulate T_h2 polarization, such as thymus-specific lymphopoietin (TSLP), OX40 ligand (OX40L) or prostaglandin (PG) E_2. In the microarray analysis of glycolipid-stimulated NKT cells and DCs, no inducible transcription of TSLP and OX40L in NKT cells was observed 1.5 or 12 h after OCH treatment. Furthermore, synthetic pathway for PGs seems quiescent because the expression of PG H synthetase (or cyclooxygenase 2), a key enzyme initiating PG synthesis, was not induced in either NKT cells or DCs after treatment with OCH. Considering that all of these molecules are regulated transcriptionally upon stimulation, the involvement of these molecules for OCH-mediated T_h2 polarization seems minimum. Taken together, the results demonstrated in this study suggest that OCH induces T_h2 predominance by a default pathway.

In summary, we have demonstrated here that OCH-mediated dominant T_h2 polarization is accomplished not only by the preferential IL-4 induction by NKT cells but also by the evasion of the secondary IFN-γ burst. This effect of OCH is due to the ineffective induction of IFN-γ and CD40L by NKT cells and the subsequent reduction of IL-12 secretion. These results demonstrate the cellular mechanisms involved in altered glycolipid ligand (OCH)-induced T_h2 polarization and immune regulation *in vivo*. Therefore, proper assessment of the effects of the innate immune system on the host's response should be taken into consideration when modulating NKT responses *in vivo* by glycolipids, such as OCH.

Acknowledgements

We thank Miho Mizuno for technical assistance and Yuki Kikai for cell sorting. We are grateful to John Ludovic Croxford for critical reading of the manuscript. This work was supported by the Pharmaceutical and Medical Devices Agency, Grant-in-Aid for Scientific Research (B) 14370169 from Japan Society for the Promotion of Science, Kato Memorial Bioscience Foundation and Uehara Memorial Foundation.

Abbreviations

APC	allophycoerythrin
CD40L	CD40 ligand
CIA	collagen-induced arthritis
DC	dendritic cell
EAE	experimental autoimmune encephalomyelitis
Flt3L	Flt3-ligand
αGC	α-Galactosylceramide
iNKT	invariant NKT
NF-κB	nuclear factor-κB
ODN	oligodeoxynucleotide
OX40L	OX40 ligand
PAMP	pathogen-associated molecular pattern
PG	prostaglandin
TSLP	thymus-specific lymphopoietin

References

1 Kronenberg, M. and Gapin, L. 2002. The unconventional lifestyle of NKT cells. *Nat. Rev. Immunol.* 2:557.
2 Taniguchi, M., Harada, M., Kojo, S., Nakayama, T. and Wakao, H. 2003. The regulatory role of Valpha14 NKT cells in innate and acquired immune response. *Annu. Rev. Immunol.* 21:483.
3 Smyth, M. J., Crowe, N. Y., Pellicci, D. G. *et al.* 2002. Sequential production of interferon-gamma by NK1.1(+) T cells and natural killer cells is essential for the antimetastatic effect of alpha-galactosylceramide. *Blood* 99:1259.
4 Singh, N., Hong, S., Scherer, D. C. *et al.* 1999. Cutting edge: activation of NK T cells by CD1d and alpha-galactosylceramide directs conventional T cells to the acquisition of a Th2 phenotype. *J. Immunol.* 163:2373.
5 Hayakawa, Y., Takeda, K., Yagita, H., Van Kaer, L., Saiki, I. and Okumura, K. 2001. Differential regulation of Th1 and Th2 functions of NKT cells by CD28 and CD40 costimulatory pathways. *J. Immunol.* 166:6012.
6 Mizuno, M., Masumura, M., Tomi, C. *et al.* 2004. Synthetic glycolipid OCH prevents insulitis and diabetes in NOD mice. *J. Autoimmun.* 23:293.
7 Chiba, A., Oki, S., Miyamoto, K., Hashimoto, H., Yamamura, T. and Miyake, S. 2004. Suppression of collagen-induced arthritis by natural killer T cell activation with OCH, a sphingosine-truncated analog of alpha-galactosylceramide. *Arthritis Rheum.* 50:305.
8 Miyamoto, K., Miyake, S. and Yamamura, T. 2001. A synthetic glycolipid prevents autoimmune encephalomyelitis by inducing TH2 bias of natural killer T cells. *Nature* 413:531.
9 Oki, S., Chiba, A., Yamamura, T. and Miyake, S. 2004. The clinical implication and molecular mechanism of preferential IL-4 production by modified glycolipid-stimulated NKT cells. *J. Clin. Investig.* 113:1631.
10 Carnaud, C., Lee, D., Donnars, O. *et al.* 1999. Cross-talk between cells of the innate immune system: NKT cells rapidly activate NK cells. *J. Immunol.* 163:4647.
11 Fujii, S. I., Shimizu, K., Smith, C., Bonifaz, L. and Steinman, R. M. 2003. Activation of natural killer T cells by {alpha}-galactosylceramide rapidly induces the full maturation of dendritic cells *in vivo* and thereby acts as an adjuvant for combined CD4 and CD8 T cell immunity to a coadministered protein. *J. Exp. Med.* 198:267.
12 Hermans, I. F., Silk, J. D., Gileadi, U. *et al.* 2003. NKT cells enhance CD4+ and CD8+ T cell responses to soluble antigen *in vivo* through direct interaction with dendritic cells. *J. Immunol.* 171:5140.
13 Kitamura, H., Ohta, A., Sekimoto, M. *et al.* 2000. Alpha-galactosylceramide induces early B-cell activation through IL-4 production by NKT cells. *Cell Immunol.* 199:37.
14 Schmieg, J., Yang, G., Franck, R. W. and Tsuji, M. 2003. Superior protection against malaria and melanoma metastases by a C-glycoside analogue of the natural killer T cell ligand alpha-galactosylceramide. *J. Exp. Med.* 198:1631.
15 Vincent, M. S., Leslie, D. S., Gumperz, J. E., Xiong, X., Grant, E. P. and Brenner, M. B. 2002. CD1-dependent dendritic cell instruction. *Nat. Immunol.* 3:1163.
16 Tomura, M., Yu, W. G., Ahn, H. J. *et al.* 1999. A novel function of Valpha14+CD4+NKT cells: stimulation of IL-12 production by antigen-presenting cells in the innate immune system. *J. Immunol.* 163:93.
17 Brigl, M., Bry, L., Kent, S. C., Gumperz, J. E. and Brenner, M. B. 2003. Mechanism of CD1d-restricted natural killer T cell activation during microbial infection. *Nat. Immunol.* 4:1230.
18 Gilliet, M., Boonstra, A., Paturel, C. *et al.* 2002. The development of murine plasmacytoid dendritic cell precursors is differentially regulated by FLT3-ligand and granulocyte/macrophage colony-stimulating factor. *J. Exp. Med.* 195:953.
19 Chiba, A., Kaieda, S., Oki, S., Yamamura, T. and Miyake, S. 2005. The involvement of V(alpha)14 natural killer T cells in the pathogenesis of arthritis in murine models. *Arthritis Rheum.* 52:1941.
20 Pal, E., Tabira, T., Kawano, T., Taniguchi, M., Miyake, S. and Yamamura, T. 2001. Costimulation-dependent modulation of experimental autoimmune encephalomyelitis by ligand stimulation of V alpha 14 NK T cells. *J. Immunol.* 166:662.
21 Kitamura, H., Iwakabe, K., Yahata, T. *et al.* 1999. The natural killer T (NKT) cell ligand alpha-galactosylceramide demonstrates its immunopotentiating effect by inducing interleukin (IL)-12 production by dendritic cells and IL-12 receptor expression on NKT cells. *J. Exp. Med.* 189:1121.
22 Trinchieri, G. 2003. Interleukin-12 and the regulation of innate resistance and adaptive immunity. *Nat. Rev. Immunol.* 3:133.
23 Schulz, O., Edwards, A. D., Schito, M. *et al.* 2000. CD40 triggering of heterodimeric IL-12 p70 production by dendritic cells *in vivo* requires a microbial priming signal. *Immunity* 13:453.
24 Hilkens, C. M., Kalinski, P., de Boer, M. and Kapsenberg, M. L. 1997. Human dendritic cells require exogenous interleukin-12-inducing factors to direct the development of naive T-helper cells toward the Th1 phenotype. *Blood* 90:1920.
25 Vieira, P. L., de Jong, E. C., Wierenga, E. A., Kapsenberg, M. L. and Kalinski, P. 2000. Development of Th1-inducing capacity in myeloid dendritic cells requires environmental instruction. *J. Immunol.* 164:4507.
26 Snijders, A., Kalinski, P., Hilkens, C. M. and Kapsenberg, M. L. 1998. High-level IL-12 production by human dendritic cells requires two signals. *Int. Immunol.* 10:1593.
27 Klinman, D. M. 2004. Immunotherapeutic uses of CpG oligodeoxynucleotides. *Nat. Rev. Immunol.* 4:249.
28 Krug, A., Towarowski, A., Britsch, S. *et al.* 2001. Toll-like receptor expression reveals CpG DNA as a unique microbial stimulus for plasmacytoid dendritic cells which synergizes with CD40 ligand to induce high amounts of IL-12. *Eur. J. Immunol.* 31:3026.
29 Parekh, V. V., Singh, A. K., Wilson, M. T. *et al.* 2004. Quantitative and qualitative differences in the *in vivo* response of NKT cells to distinct alpha- and beta-anomeric glycolipids. *J. Immunol.* 173:3693.
30 Goff, R. D., Gao, Y., Mattner, J. *et al.* 2004. Effects of lipid chain lengths in alpha-galactosylceramides on cytokine release by natural killer T cells. *J. Am. Chem. Soc.* 126:13602.
31 Smyth, M. J., Thia, K. Y., Street, S. E. *et al.* 2000. Differential tumor surveillance by natural killer (NK) and NKT cells. *J. Exp. Med.* 191:661.
32 Whiteside, T. L. and Herberman, R. B. 1995. The role of natural killer cells in immune surveillance of cancer. *Curr. Opin. Immunol.* 7:704.
33 Ortaldo, J. R., Young, H. A., Winkler-Pickett, R. T., Bere, E. W., Jr. Murphy, W. J. and Wiltrout, R. H. 2004. Dissociation of NKT stimulation, cytokine induction, and NK activation *in vivo* by the use of distinct TCR-binding ceramides. *J. Immunol.* 172:943.

34 Ueno, Y., Tanaka, S., Sumii, M. *et al.* 2005. Single dose of OCH improves mucosal T helper type 1/T helper type 2 cytokine balance and prevents experimental colitis in the presence of valpha14 natural killer T cells in mice. *Inflamm. Bowel Dis.* 11:35.
35 Cella, M., Scheidegger, D., Palmer-Lehmann, K., Lane, P., Lanzavecchia, A. and Alber, G. 1996. Ligation of CD40 on dendritic cells triggers production of high levels of interleukin-12 and enhances T cell stimulatory capacity: T-T help via APC activation. *J. Exp. Med.* 184:747.
36 Quezada, S. A., Jarvinen, L. Z., Lind, E. F. and Noelle, R. J. 2004. CD40/CD154 interactions at the interface of tolerance and immunity. *Annu. Rev. Immunol.* 22:307.
37 Hayes, M. P., Murphy, F. J. and Burd, P. R. 1998. Interferon-gamma-dependent inducible expression of the human interleukin-12 p35 gene in monocytes initiates from a TATA-containing promoter distinct from the CpG-rich promoter active in Epstein–Barr virus-transformed lymphoblastoid cells. *Blood* 91:4645.
38 Ma, X., Chow, J. M., Gri, G. *et al.* 1996. The interleukin 12 p40 gene promoter is primed by interferon gamma in monocytic cells. *J. Exp. Med.* 183:147.
39 Grohmann, U., Belladonna, M. L., Bianchi, R. *et al.* 1998. IL-12 acts directly on DC to promote nuclear localization of NF-kappaB and primes DC for IL-12 production. *Immunity* 9:315.
40 Gumperz, J. E. 2004. CD1d-restricted NKT cells and myeloid IL-12 production: an immunological crossroads leading to promotion or suppression of effective anti-tumor immune responses? *J. Leukoc. Biol.* 76:307.

Therapeutic Potential of Glycolipid Ligands for Natural Killer (NK) T Cells in the Suppression of Autoimmune Diseases

Sachiko Miyake* and Takashi Yamamura

Department of Immunology, National Institute of Neuroscience, NCNP, 4-1-1 Ogawahigashi, Kodaira, Tokyo 187-8502, Japan

Abstract: NKT cells emerge as important regulatory cells in autoimmune responses. Abnormalities in the numbers and functions of natural killer T (NKT) cells have been observed in patients with autoimmune diseases as well as in a variety of mouse strains that are genetically predisposed for development of autoimmune diseases. Unlike conventional T cells that recognize peptides in association with major histocompatibility complex (MHC), NKT cells recognize glycolipid antigens presented by the non-polymorphic MHC class I-like protein, CD1d. Recently, we and other groups have demonstrated that administration of glycolipid ligands such as α-galactosylceramide (α-GC) or its sphingosine truncated derivative, OCH suppressed autoimmune diseases such as experimental autoimmune encephalomyelitis (EAE), diabetes in NOD mice and collagen-induced arthritis (CIA) by inducing T helper (Th) 2 bias of autoimmune T cells. OCH is a unique ligand to stimulate NKT cells to selectively produce Th2 cytokines whereas α-GC induces both interleukin (IL)-4 and interferon (IFN)-γ, and is more beneficial for treatment of a wide variety of Th1-mediated autoimmune diseases. The lack of polymorphism of CD1d and cross-reactive responses of mouse and human NKT cells to the same ligand indicates that targeting NKT cells with this ligand may be an attractive means for intervening in human autoimmune diseases such as type I diabetes (T1D), multiple sclerosis (MS) and rheumatoid arthritis (RA).

The present review will focus on the potential roles of NKT cells in the pathogenesis of autoimmune diseases and the recent advances in glycolipid therapy for autoimmune disease models. The molecular mechanism of OCH-induced Th2-selective cytokine secretion will also be discussed.

Key Words: NKT cell, CD1, α-galactosylceramide, OCH, autoimmune disease, therapy, Th1/Th2.

INTRODUCTION

Autoimmunity has been studied for more than four decades, but its pathogenesis has remained a mystery. Despite that, potent new biologic therapeutics including cytokines and anti-cytokine reagents show remarkable clinical efficacy in several autoimmune diseases such as MS and RA. However, these drugs have limited value at best, and sometimes are accompanied by serious side effects. Thus drug development for these autoimmune diseases is a fundamental challenge in the 21st century.

It is well-established that central tolerance, the deletion of T cells with high avidity for self-antigens restricts the repertoire of peripheral auto-reactive T cells. However, this process is incomplete. Lymphocytes with lower avidity for self-antigens, or with high avidity for determinants that are not expressed in the thymus (self or foreign), are found in the periphery. The presence of peripheral T cells that react with self-antigens in healthy individuals indicates the existence of physiological regulatory mechanisms that prevent pathological autoimmunity. Such control is referred to as peripheral tolerance, and peripheral tolerance comprises pathways that act directly on auto-reactive cells (intrinsic tolerance: ignorance, anergy, phenotypic skewing) or indirectly through cells such as $CD4^+CD25^+$ T cells and NKT cells [1]. Disruption of these tolerance mechanisms could lead to autoimmune disease. Conversely, maintenance or re-establishment of peripheral tolerance is a therapeutic strategy to restrain destructive autoimmune processes. Thus it seems attractive to induce or stimulate regulatory cells to control harmful autoimmunity [2,3]. Among several different regulatory cells, we would like to focus on targeting NKT cells, because a number of recent studies suggest NKT cells are involved in the pathogenesis of autoimmunity. In addition, several glycolipid ligands can selectively stimulate NKT cells and have been shown to prevent autoimmune disease models.

NKT CELLS AND THEIR ANTIGENS

NKT cells are usually defined as cells co-expressing of the natural killer receptors such as NK1.1 or NKR-P1A (CD161) and a αβ T cell receptor (TCR). Although $NK1.1^+$ TCR^+ lymphocytes are heterogeneous, most NKT cells express an invariant TCRα chain composed of Vα14-Jα18 segments in mice and Vα24-Jα18 segments in humans, which is associated with TCR β chains using a restricted set of Vβ genes. These Vα14 invariant NKT cells recognize glycolipid antigens such as α−GC presented by a nonpolymorphic MHC class I-like molecule, CD1d [4,5]. As little is known about CD1d non-restricted NKT cells or α-GC independent CD1d restricted NKT cells, in this review we focus on the α-GC responsive NKT cells, and "NKT cells" will be used for α-GC responsive NKT cells.

*Address correspondence to this author at the Department of Immunology, National Institute of Neuroscience, NCNP, 4-1-1 Ogawahigashi, Kodaira, Tokyo 187-8502, Japan; Tel: +81-42-341-2711; Fax: +81-42-346-1753; E-mail: miyake@ncnp.go.jp

1568-0088/05 $50.00+.00